NASA TN D-182

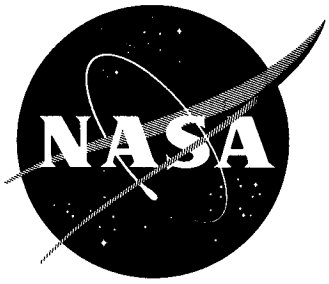

TECHNICAL NOTE
D-182

INVESTIGATION OF IGNITION TEMPERATURES OF SOLID METALS

By W. C. Reynolds

Stanford University

NATIONAL AERONAUTICS AND SPACE ADMINISTRATION

WASHINGTON

October 1959

NATIONAL AERONAUTICS AND SPACE ADMINISTRATION

TECHNICAL NOTE D-182

INVESTIGATION OF IGNITION TEMPERATURES OF SOLID METALS

By W. C. Reynolds

SUMMARY

The ignition temperature of a solid metal is related through a thermal definition of ignition to the rate of oxidation and to the radiation and convection heat-transfer parameters. The mechanisms of oxidation are reviewed and the factors which influence ignition temperatures are discussed. Reasonable agreement between theoretical and experimental ignition temperatures is demonstrated. Experimental ignition temperatures for several metals are presented.

INTRODUCTION

For many years the maximum safe operating temperatures for metals have been determined from strength considerations. However, some metals have been known to ignite and burn at what would normally be structurally safe temperatures. It seems, then, that failure by ignition and burning may, in some cases, precede failure by structural weakening with temperature and that the possibility of ignition must be considered in the design of high-temperature metal apparatus.

The advent of high-speed flight has brought about increased interest in the problem of metal ignition. At flight speeds typical of modern aircraft and missiles, aerodynamic heating causes extremely high skin temperatures. The danger of ignition is increased in regions behind shock waves where temperatures and pressures are exceptionally high. Other fields where metal ignition is of interest include the design of gas turbines, high-temperature furnaces, gas-cooled nuclear reactors, and rocket motors.

Obviously there are many factors which enter into the problem of ignition and burning. The mechanisms involved are entirely different, and the distinction between ignition and burning must be kept clear. Ignition is brought about by the exothermal oxidation reaction between the solid metal and its gaseous environment. Consequently, it is believed that the phenomenon of ignition is quite closely related to the relatively slow oxidation that occurs on all metals at low temperatures ("rusting"). Burning, on the other hand, may proceed by any of

several mechanisms. It may be a surface reaction, that is, a further extension of the rusting process; the burning of many metals, notably magnesium, is a vapor-phase reaction and occurs at some distance from the surface. It is conceivable that a body could ignite but not burn, the ignition (rise in temperature) leading simply to melting. This investigation is concerned primarily with the problem of ignition. However, it is impossible to divorce completely ignition from burning, and so some attention has been given to the latter phenomenon also.

Very little information regarding the ignition of metals is available. However, a great deal of information is known about the oxidation of metals. It is not unreasonable to expect that the heat generated in the oxidation reaction prior to ignition could be calculated from oxidation data extrapolated to temperatures near ignition. Under this assumption an ignition temperature may be defined and calculated. For metals where the extrapolation is not made over too large a temperature difference, reasonable agreement between calculated and experimental ignition temperatures can be obtained. The effect of varying the environmental conditions can then be studied. A great deal is known about the mechanisms of oxidation, and thus a study of these mechanisms gives considerable insight into the ignition problem.

The primary objective of this investigation is to study the effects of important environmental parameters on the ignition temperatures of solid metals. Considerable effort has been devoted to the study of the mechanisms of oxidation and to the relation of these phenomena to ignition. Thus, the investigation is primarily one of a theoretical nature, but a certain amount of data has been gathered to confirm and supplement the knowledge of the ignition mechanisms. Since one of the most important applications of this research is in the high-speed flight problem, special attention has been given to metals of interest in aircraft construction. It is difficult to produce flight conditions of this nature in the laboratory, and therefore attention has been given to the manner in which flight conditions (flow velocity, gas pressure and temperature, heat transfer, etc.) influence the oxidation rate and the ignition temperatures.

The present investigation was carried out at Stanford University under the sponsorship and with the financial assistance of the National Advisory Committee for Aeronautics.

SYMBOLS

A	action constant, g/cm^2-sec or g^2/cm^4-sec; area, cm^2 or ft^2; constant, dimensional as defined where used
a	constant

B	constant, dimensional as defined where used
C	constant, dimensional as defined where used; thermal capacitance, cal/^{o}K or Btu/^{o}F
C_a	number of activated adsorption sites, 1/cm^2
D	diffusion coefficient, cm^2/sec; diameter, cm, ft, or in.
E	activation energy, cal/mole; constant, dimensional as defined where used
F	Faraday's constant, 96,500 coulombs/(g equivalent)
F^*	Faraday's constant, 23,066 cal/volt
$\mathscr{F}$	dimensionless factor, defined where used
f	dimensionless factor, defined where used
h	heat-transfer coefficient, cal/sec-cm^2-^{o}C or Btu/hr-ft^2-^{o}F
$\hbar$	Planck's constant, 6.624×10^{-27} erg sec
K	rate constant, g/(cm^2-sec) or g^2/(cm^4-sec)
l	electrical conductivity of a single mode, 1/ohm-cm
M	Mach number
m	mass of molecule or atom, g
m	factor, defined where used
N_{Re}	Reynolds number
N_o	Avogadro's number, 6.023×10^{23} per mole
n	constant; molecular concentration per unit volume, molecules/cm^3
p	pressure, dynes/cm^2, atm, or lb/ft^2
Q	heat of reaction per gram of oxygen, cal/g
q"	heat-transfer rate per unit area, cal/sec-cm^2 or Btu/hr-ft^2
R	universal gas constant, 1.986 cal/mole

r	ratio of volume of oxide to volume of metal
T	absolute temperature, ^{o}K or ^{o}R
V	volume, cm^3
v	velocity of molecular reaction, molecules/sec
W	molecular weight
w	weight of oxygen reacted with metal, g
x	coordinate, cm
z	atomic weight of oxide, g/mole
α	factor, defined where used
Γ	rate of molecular diffusion per unit area, molecules/cm^2-sec
γ	ratio of mass of oxide to mass of oxygen forming it
δ	thickness of oxide film, cm; thickness of boundary layer, cm or in.
ϵ	emissivity
θ	time, sec
κ	Boltzmann's constant, 1.380×10^{-16} erg/^{o}K
λ	free molecular path, cm
λ_m	mean free molecular path, cm
ξ	coordinate, cm
ρ	density, g/cm^3 or lb/ft^3
σ	Stefan-Boltzmann constant, 13.77×10^{-13} cal/cm^2-sec-$^{o}K^4$ or 17.13×10^{-12} Btu/hr-ft^2-$^{o}R^4$; molecular or atomic diameter, cm
τ	transference numbers for electrical conductivity
η	pyrophoricity
η_l	linear pyrophoricity, $\frac{A_l Q}{4\sigma\epsilon}\left(\frac{R}{E_l}\right)^4$

η_p parabolic pyrophoricity, $\frac{A_p Q}{8\sigma\epsilon\delta\rho_{oxide}\gamma}\left(\frac{R}{E_p}\right)^4$

h^* term characterizing convection heat transfer

h_l^* linear heat transfer, $\frac{h}{A_l Q}\frac{E_l}{R}$

h_p^* parabolic heat transfer, $\frac{2h\delta\rho_{oxide}\gamma}{A_p Q}\frac{E_p}{R}$

T^* ignition temperature

T_l^* linear ignition temperature, RT_{ig}/E_l

T_p^* parabolic ignition temperature, RT_{ig}/E_p

Subscripts:

o refers to ambient (T_o denotes recovery temperature), or denotes heating independent of temperature

1 refers to oxygen in the gaseous environment, or defined where used

2 refers to inert gases in the environment, or defined where used

3 refers to oxide vapor

∞ refers to ambient or environment

A refers to anion

C refers to cation

e refers to electron

ig used to denote ignition temperature

iso isothermal

l refers to linear oxidation

m	refers to metal
ox	refers to oxidation
oxide	refers to oxide
p	refers to parabolic oxidation
s	used to denote surface temperature
sat	saturated

RELATION BETWEEN IGNITION TEMPERATURE AND OXIDATION RATE

Thermal Definition of Ignition

Before any sensible approach to the problem of solid-body ignition can be made, the ignition temperature must be defined. Generally, ignition is said to occur when the body temperature rises spontaneously and a self-propagating reaction occurs at some elevated temperature. Evidently, thermal stability is involved, and the definition of ignition must be obtained through energy considerations. An energy balance on an object of arbitrary shape results in a complex partial-differential equation, the solution of which describes the temperature-time history of every point in the object. Ignition will occur when, at some point in the object, the temperature starts to rise rapidly, that is, when the heating effect of the exothernal oxidation reaction overcomes the conduction, convection, and radiation cooling. A general definition of ignition, even in the case of simple shapes, involves the solution of the highly nonlinear energy equation and is impractical. If the conduction terms in the energy equation are momentarily overlooked, an analysis can be made, and the ignition temperature can be expressed mathematically. Such an analysis then allows an examination of how the ignition temperature depends on environmental conditions. The trends thus indicated should be similar to those applying to more complex systems. Such a simple analysis is therefore of great value, but the assumptions involved must be remembered.

The thermal definition of ignition introduced here is based on an energy balance on an oxidizing isothermal body of arbitrary shape, cooled by convection and radiation. If it is assumed that the heat generated in the reaction may be treated as a heat addition at the surface and that the oxidation, convection, and radiation heat-transfer rates are uniform over the surface, an energy balance on the isothermal body gives

$$\frac{C}{A}\frac{dT}{d\theta} = q''_{ox} - h\left(T - T_o\right) - \sigma\epsilon\left(T^4 - T_\infty^4\right) + q''_o = \phi(T) \qquad (1)$$

where q''_o is any heat input independent of the body temperature. Note that the rate of change of the body temperature is a function of the temperature and several environmental parameters assumed to be constants. Note that the same equation would apply if the convection and radiation heat-transfer terms were treated as heating rather than cooling terms.

The temperature-time history of the body can be found by integration of equation (1). If the temperature tends to increase in time and the environmental parameters are constant, the body will eventually reach a "steady-state" condition under which the heat input due to oxidation (and perhaps electrical energy) is balanced by the convective and radiation cooling. For most metals, as the temperature increases, the reaction rate increases nearly exponentially and, therefore, q''_{ox} is usually a rather rapidly increasing function of temperature. This tends to be offset by the increase in the convective and radiation cooling with increasing temperature. Under normal conditions the temperature will rise at a decreasing rate to the point at which the heat inputs are exactly balanced by the cooling, and the body will remain at this steady-state temperature indefinitely. However, if the temperature reaches a point at which further increase in temperature will result in an increase in the oxidation heat input larger than the increase in cooling, the body temperature will then continue to rise at an increasing rate and no steady-state condition will be reached. It appears, then, that there is a maximum steady-state temperature at which the body can exist indefinitely. This temperature is seen to be a function of the environmental conditions. If, in the course of a thermal transient, the temperature should exceed this limit, then the temperature would continue to rise until melting or full-scale combustion phenomena occurred. This maximum stable steady-state temperature will henceforth be called the ignition temperature. Note that ignition as defined here is not necessarily followed by burning; melting produced by the temperature rise due to oxidation could alter the oxidation characteristics sufficiently to prevent further temperature rise to the point of vaporization and actual combustion.

On the basis of the foregoing arguments, the ignition temperature is seen to be equivalent to the temperature at which the body temperature begins to increase at an increasing rate. This may be expressed mathematically as the temperature at which $dT/d\theta$ is a minimum, as seen in the following sketch:

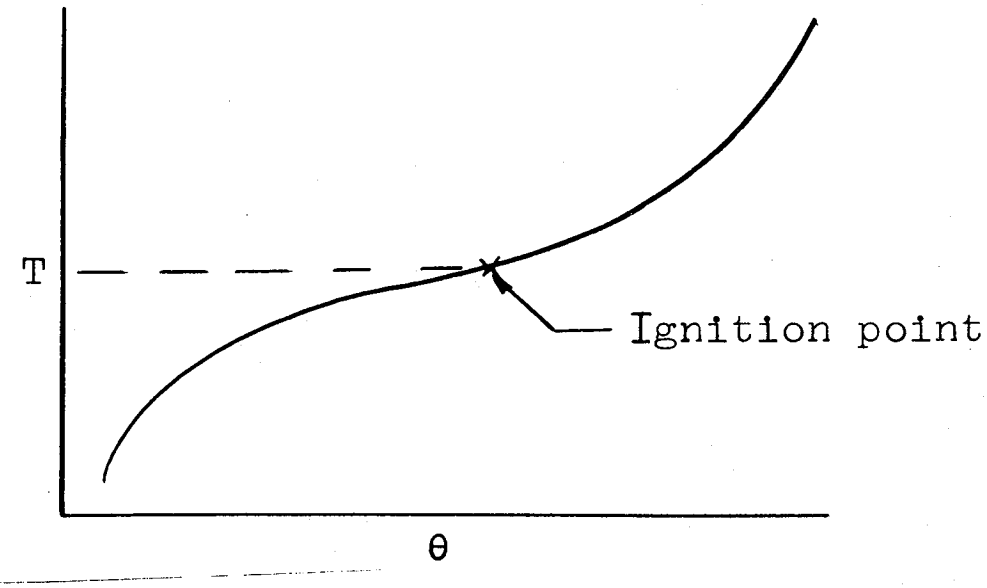

The ignition temperature can be found as a function of the environmental and oxidation parameters by requiring that the derivative of equation (1) with respect to temperature vanish. The resulting defining equation for the ignition temperature is

$$\left[\frac{d}{dT}\left(q''_{ox}\right)\right]_{T=T_{ig}} - h - 4\sigma\epsilon T_{ig}^{3} = 0 \qquad (2)$$

It should be noted that, for ignition to occur, $dT/d\theta$ must be positive at the ignition temperature, and the dependence of the oxidation rate on temperature must be positive and stronger than that of the dominating cooling term. It is extremely interesting that, unless the oxidation rate depends on ambient temperature, the ignition temperature is independent of ambient temperature.

Oxidation-Rate Equations

In general, the oxidation behavior of technically important metals can be classified as either linear or parabolic and correlated by equations of the form

$$w = A_l e^{-E_l/RT}\theta = K_l\theta \qquad (3)$$

for linear oxidation and

$$w^2 = A_p e^{-E_p/RT} \theta = K_p \theta \tag{4}$$

for parabolic oxidation. In these empirical fits to observed data, w is the weight of oxygen per unit of surface area that has reacted with the metal in time θ; K is referred to as the rate constant; E is referred to as the activation energy; and A is referred to as the action constant. The constants A and E, in general, depend on environmental conditions and may even be functions of the metal temperature. The constants are obtained from experimental data by plotting the logarithm of K against $1/T$; E is first determined from the slope of a line through the data points, and then A is easily calculated. Since the exponent E/RT is usually relatively high (10 to 80), any small error in E due to fitting a straight line through experimental points causes a large error in A. Even the most careful experimenters in the field of metal oxidation estimate the uncertainty in their activation energies as ±5,000 calories in about 40,000 calories, and thus the uncertainty in A may be an order of magnitude. This high uncertainty in the oxidation constants limits any quantitative attempt to predict ignition temperatures from experimental oxidation data. Nevertheless, by studying the manner in which these constants depend on environmental conditions, a great deal can be learned about how ignition temperatures depend on environment. Experimental values of A and E for a number of metals are given in table 1. These data are taken largely from reference 2.

The rate of heat generation per unit area is obtained by differentiating equations (3) or (4) with respect to time and multiplying by the heat of reaction per gram of oxygen. This yields

$$q''_{ox} = QA_l e^{-E_l/RT} \tag{5}$$

for linear oxidation and

$$q''_{ox} = \frac{QA_p}{2\delta\rho_{oxide}\gamma} e^{-E_p/RT} \tag{6}$$

for parabolic oxidation.

The introduction of equation (5) into equation (2) allows expression of the ignition temperature for linearly oxidizing metals in the following explicit form:

$$e^{-1/T_l^*} = \frac{(T_l^*)^5}{\eta_l} + h_l^* (T_l^*)^2 \tag{7}$$

where

$$T_l^* = T_{ig}R/E_l$$

$$\eta_l = \frac{A_l Q}{4\sigma\epsilon}\left(\frac{R}{E_l}\right)^4$$

$$h_l^* = \frac{h}{A_l Q}\frac{E_l}{R}$$

Similarly, upon substitution of equation (6) into equation (2) there results the following expression for the ignition temperature of parabolically oxidizing metals:

$$e^{-1/T_p^*} = (1/\eta_p)(T_p^*)^5 + h_p^*(T_p^*)^2 \qquad (8)$$

where

$$T_p^* = T_{ig}R/E_p$$

$$\eta_p = \frac{A_p Q}{8\sigma\epsilon\delta\rho_{oxide}\gamma}\left(\frac{R}{E_p}\right)^4$$

$$h_p^* = \frac{2h\delta\rho_{oxide}\gamma}{A_p Q}\frac{E_p}{R}$$

Since equations (7) and (8) are of the same form, a single set of curves may be used to represent the solution of both. Figure 1 shows the dimensionless ignition temperature T^* plotted against η with h^* as a parameter. Hereafter η will be referred to as the pyrophoricity; note that materials having high pyrophoricities will have relatively low ignition temperatures. Note also that the effect of an increase in the rate of convective heat transfer, either heating or cooling, will tend to give higher ignition temperatures. This result is quite surprising and as yet has not been supported or repudiated by experimental data. It must be remembered that the oxidation-rate constants A and E may depend on environmental conditions, in which case the ignition temperature is said to depend indirectly on environment.

MECHANISMS OF METAL OXIDATION

In order to investigate the manner in which the ignition temperature depends on environmental conditions, it is necessary to understand the mechanisms of the oxidation reaction. It is well known that the oxidation reaction proceeds by a series of steps, the slowest of which controls the overall rate of reaction. By comparison of the relative rates of occurrence of these steps it appears that only three of these may be slow enough to be rate controlling: namely, (1) the rate of transport of oxygen to the reacting surface, (2) the rate of adsorption of oxygen molecules at the surface, and (3) the rate of diffusion of ions in the oxide. Analysis indicates that, if the oxygen transport rate controls the reaction, the surface will become oxygen starved, and the body will not ignite. Such a situation might occur on an aircraft flying at extremely high altitudes or on a body sitting in very still air. The oxidation of some metals, notably magnesium and magnesium alloys, is believed to be controlled by the rate of oxygen adsorption. The rate of adsorption is not influenced by ambient pressure, except at extremely low pressures; at low pressures the oxidation rate is decreased, resulting in an increase in the ignition temperature. In continuum flows the adsorption rate is practically independent of the ambient temperature, but in noncontinuum flows the adsorption rate may be very strongly influenced by the gas temperature, being accelerated when the ambient temperature exceeds the body temperature. At low temperatures the oxidation of most metals is controlled by the rate of diffusion of ions in the oxide lattice. Generally, the oxidation rate is independent of ambient temperature and only mildly dependent on the ambient pressure but it may either increase or decrease with increased pressure, depending on the particular mechanism of ion diffusion involved. The rate of ion diffusion varies inversely as the thickness of the oxide scale. Thus it is possible that the removal of the bulk of the oxide scale by the drag of airflow over the surface may substantially increase the oxidation rate and thus lower the ignition temperature.

The mechanisms which govern the oxidation of a given metal will depend on the environment; for example, the rate of oxygen transport will certainly control the oxidation of the skin of a missile flying at 500,000 feet, whereas the sea-level oxidation rate will be controlled by either adsorption or ion diffusion, depending on the relative rates of these two processes.

The mechanisms of oxidation, the rates of oxidation, and the influence of environmental conditions of each are summarized in table 2.

Steps in Oxidation Reaction

For the purposes of this discussion, a simple model of a pure metal Me having valence 2x+ and forming a single oxide MeO_x is used. This model is shown as follows (the various steps in the reaction are numbered):

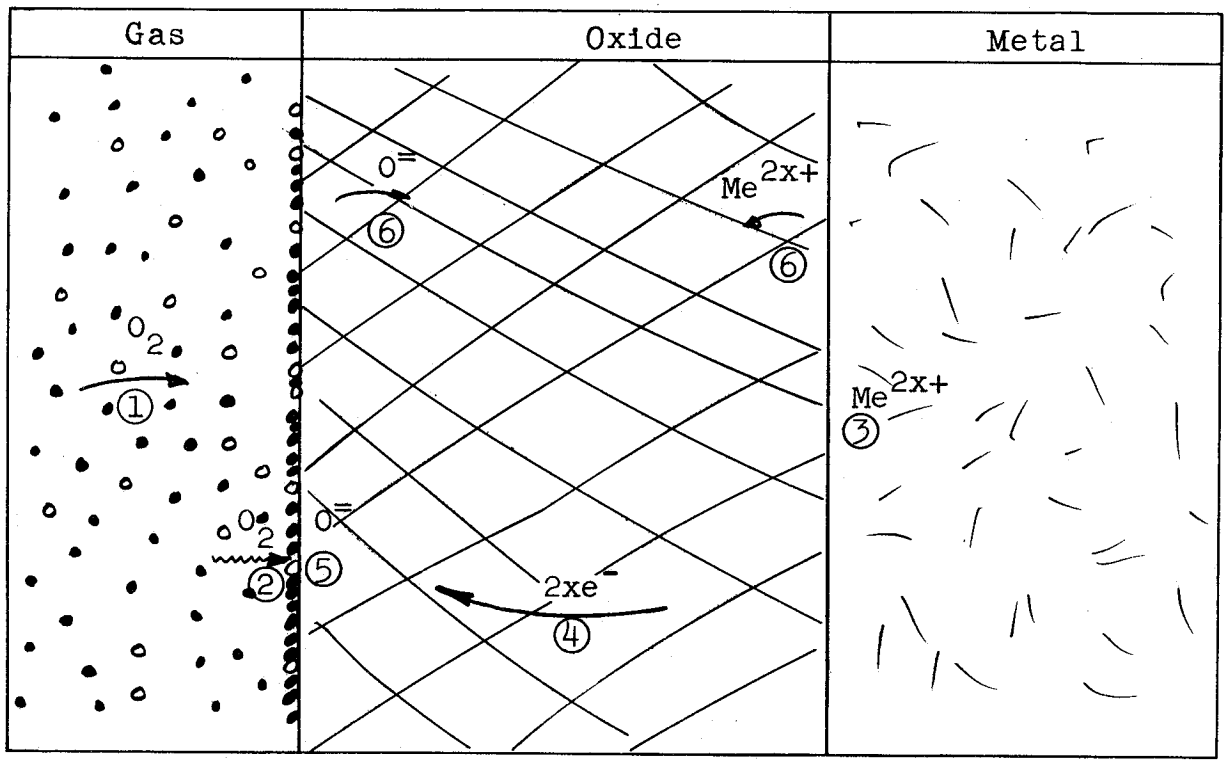

The black dots represent oxygen molecules, and the small circles represent molecules of inert gas present in the gaseous environment. The $2xe^-$ indicates the number of electrons transferred in the ionization of stoichiometric amounts of metal and oxygen.

The steps which occur in the oxidation reaction are numbered and are as follows:

(1) Oxygen molecules are transported to the gas-oxide interface by forced or natural diffusion through the inert gas molecules.

(2) Oxygen molecules whose energy exceeds a certain level are adsorbed by the surface of the oxide.

(3) Metal atoms ionize at the metal-oxide interface.

(4) The electrons given up by the metal atoms diffuse through the oxide lattice to the gas-oxide interface.

(5) The oxygen molecules dissociate, and oxygen atoms are ionized by the electrons.

(6) The oxygen and metal ions diffuse in the oxide lattice, meeting and falling into place in the crystal structure.

Each of these steps will be discussed in detail subsequently. It must be remembered that this is an extremely simple model for analysis and many complicating factors may enter. For example, if the oxide is porous, the gas may attack the metal directly in places and thus two parallel paths for the oxidation may exist; the formation of blisters may inhibit the reaction; several oxides may be formed; and impurities or alloying elements may influence the oxidation. These complicating factors are discussed rather thoroughly in reference 2.

Of particular interest in the study of oxidation mechanisms is the ratio of the volume of the oxide to the volume of the base metal from which it is formed, $V_{oxide}/V_m = r$. It would seem that for $r < 1$ the oxide could not completely cover the metal surface, and a porous oxide surface would be formed. On the other hand, if r is greater than unity the oxide would tend to be pushed away from the surface, possibly allowing the formation of blisters. It would be expected that the porous oxide would be the less protective of the two types and that differences in the rate-controlling mechanisms may exist. Simplified models for the two types of oxide are shown below. Note that the porous oxide is shown to have a thin layer covering the entire metal surface.

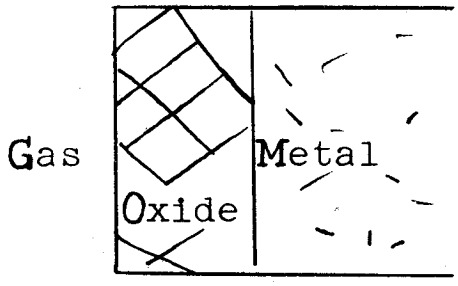

Nonporous
($r > 1$)

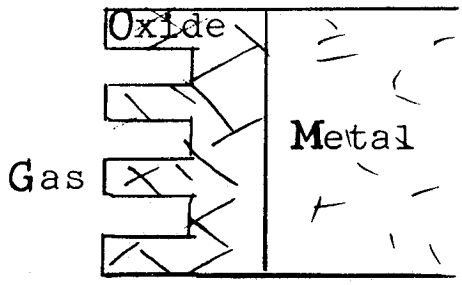

Porus
($r < 1$)

It has been observed that metals which oxidize in the parabolic manner generally form nonporous oxides, that is, $r > 1$. Moreover, metals that oxidize in the linear manner form porous oxides, $r < 1$. The reasons for this difference are not well understood. It is generally believed that diffusion through the oxide film governs the parabolic type of reactions, but there is considerable difference of opinion as to the rate-controlling step in linear oxidation. Two viewpoints that appear plausible are (1) that the rate of oxygen adsorption is the slowest step, since the film is so thin, and (2) that diffusion through a constant-thickness thin film at the roots of the pores controls the reaction.

Transport of Oxygen to Gas-Oxide Interface

As oxygen molecules are adsorbed by the oxide close to the gas-oxide interface, new molecules must be brought close to the oxide if the reaction is to be continuous. If a thermal boundary layer is formed over the surface, the temperature variation within several hundred mean free paths from the surface is essentially zero. Since nearly all the oxygen molecules which come in contact with the surface come from a region within a very few mean free paths of the surface, the gas which is transported to the surface may be considered as being at the surface temperature, regardless of the ambient temperature.

If the environment consists of pure oxygen, the rate of molecular interaction with the surface is given by kinetic theory (ref. 3) as

$$\frac{dw}{d\theta} = p\sqrt{\frac{1}{2\pi(R/W_1)T}} \tag{9}$$

where p is the oxygen pressure, W_1 is the molecular weight of oxygen, and T is the surface temperature. By inserting numerical values, it may be shown that the rate of interaction of oxygen $dw/d\theta$ is many orders of magnitude larger than observed weight gains for oxidation of metals. Moreover, the rate of interaction decreases with temperature; this temperature effect is opposite to that exhibited by metals and does not lead to an ignition condition. On the basis of these arguments it is concluded that oxygen transport does not control the rate of oxidation of metals if the environment is pure oxygen and the pressure is not too low.

If the environment contains nonreacting gases such as does air, then, as oxygen molecules are adsorbed at the surface, other oxygen molecules must diffuse through the inert gases to replace them. If the molecules are not replaced faster than they are adsorbed, the surface will become starved of oxygen, and the rate of diffusion of oxygen molecules through the inert gas to the surface would control the rate

of oxidation. The rate of oxygen-molecule diffusion through the inert gas is given by (see ref. 3)

$$\Gamma_1 = \frac{n}{n_2} D \frac{dn_1}{dx} \tag{10}$$

where n_1 is the oxygen concentration and n_2 is the inert gas concentration in molecules per unit volume $(n = n_1 + n_2)$, D is the diffusion coefficient, and x is measured from the surface. The diffusion constant D may be calculated from kinetic theory (ref. 3) as

$$D = \left[\frac{3}{2\sqrt{2}\pi(\sigma_1 + \sigma_2)^2 n}\right]\left(\frac{W_1 + W_2}{W_1 W_2} RT\right)^{1/2} \tag{11}$$

where W and σ represent the molecular weight and diffusion cross section of the respective constituents. From the perfect-gas equation of state,

$$p = n\kappa T \tag{12}$$

From consideration of the above relationships the rate of oxygen mass diffusion may be written as

$$\frac{dw}{d\theta} = \left[\frac{3m_1}{p_2 2\sqrt{2}\pi(\sigma_1 + \sigma_2)^2}\right]\left(\frac{W_1 + W_2}{W_1 W_2} RT\right)^{1/2} \frac{dp_1}{dx} \tag{13}$$

where p_1 and p_2 are the partial pressures of the oxygen and the inert gas, respectively, in the environment. For a first approximation, it may be assumed that the variation in the partial pressure of oxygen occurs in a finite region near the surface, varying from $p_{1,\infty}$ in the environment to zero at the surface. For steady diffusion $dw/d\theta$ is constant, and thus the partial pressure varies linearly from the surface as shown by the following sketch:

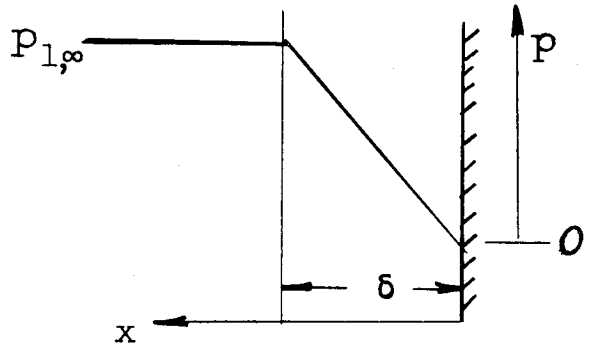

For this first approximation

$$\frac{dp_1}{dx} = \frac{p_{1,\infty}}{\delta} \tag{14}$$

δ is essentially proportional to the boundary-layer thickness, or inversely proportional to $\sqrt{N_{Re}}$ for a laminar layer. (If natural convection exists, δ will vary as the fourth root of the Grashof number.) The diffusion cross sections σ_1 and σ_2 are essentially constant. Thus, approximately,

$$\frac{dw}{d\theta} = \text{Constant} \frac{p_{1,\infty}}{p_2} \sqrt{T} \sqrt{N_{Re}} \tag{15}$$

This relationship shows the behavior of the rate of oxygen transport to the surface in a mixed-gas environment. It is seen that as the oxygen concentration becomes very small relative to the concentration of the inert gases, the rate of transport becomes very small and could conceivably be the oxidation-rate-controlling process. However, the oxidation reaction could not lead to ignition because of the very mild dependence on temperature. It therefore appears that if ignition does occur, the rate of oxygen transport is not the rate-controlling step.

The possibility that metals can be oxygen starved can be investigated by order-of-magnitude calculations. As an example, the rates of transport in air can be compared with measured oxidation rates for iron. The comparison indicates that transport does not control the reaction rate at low temperatures but may be controlling at high temperatures. For the purposes of these calculations it will be assumed that the thickness of the starved layer is 0.1 centimeter and that the partial pressure of the oxygen in the environment is 0.2 atmosphere. The diffusion coefficient for oxygen in air at 32° F is given in reference 4 as 0.178 cm^2/sec. Equation (11) indicates that the diffusion coefficient varies as the 3/2 power of the absolute temperature; thus, at 932° F, $D = 0.278$ cm^2/sec, and at $2{,}192^\circ$ F, $D = 2.23$ cm^2/sec. The partial oxygen densities at these temperatures are 1.10 and 0.528×10^{-4} g/cm^3, respectively. Thus, the transport rates are

$$\frac{dw}{d\theta} = D \frac{dp}{dx} \approx 0.278 \frac{1.10 \times 10^{-4}}{0.1} = 3.1 \times 10^{-4} g/cm^2\text{-sec}$$

at 932° F and

$$\frac{dw}{d\theta} \approx 2.2 \frac{0.528 \times 10^{-4}}{0.1} = 1.2 \times 10^{-4} g/cm^2\text{-sec}$$

at 2,192° F. Using the oxidation-rate constants of table 1 and assuming an oxide film thickness of 0.01 centimeter, the rate of oxidation of iron may be calculated as

$$\frac{dw}{d\theta} = 6.6 \times 10^{-7} g/cm^2\text{-sec}$$

at 932° F and as

$$\frac{dw}{d\theta} = 1.6 \times 10^{-4} g/cm^2\text{-sec}$$

at 2,192° F. It is seen that the transport rate at 932° F is several orders of magnitude larger than the observed oxidation rates, but at 2,192° F the transport rate may indeed be rate controlling. It seems, that transport of this type may be rate controlling at high temperatures, and thus a metal surface might become oxygen starved in air. Flow velocity would then be an extremely important parameter in the oxidation and ignition phenomena.

In the foregoing discussions it was assumed that the vapor pressures of the metals and their oxides are negligible at temperatures below ignition. This is generally true for most metals. However, certain metals and oxides, notably magnesium, molybdenum trioxide, and tungsten dioxide, have extremely high vapor pressures. The dependency of vapor pressure on temperature can usually be represented by empirical equations of the form

$$p_3 = Be^{-C/T} \tag{16}$$

Consider first the case where the vapor pressure of the oxide is high and the environment contains only oxygen. For the purpose of this discussion it will be assumed that, since the oxide vapor is continually being carried away by the boundary layer over the surface, the concentration of the vapor varies from saturation at the surface to zero at some finite distance from the surface. This distance might correspond to the thickness of the boundary layer over the surface. Oxygen must diffuse through the oxide vapor to reach the surface, and thus the oxygen concentration may be assumed to vary from zero at the surface to its free-stream value. Under these relatively simple assumptions the oxide and oxygen concentrations would appear as shown in the following sketch:

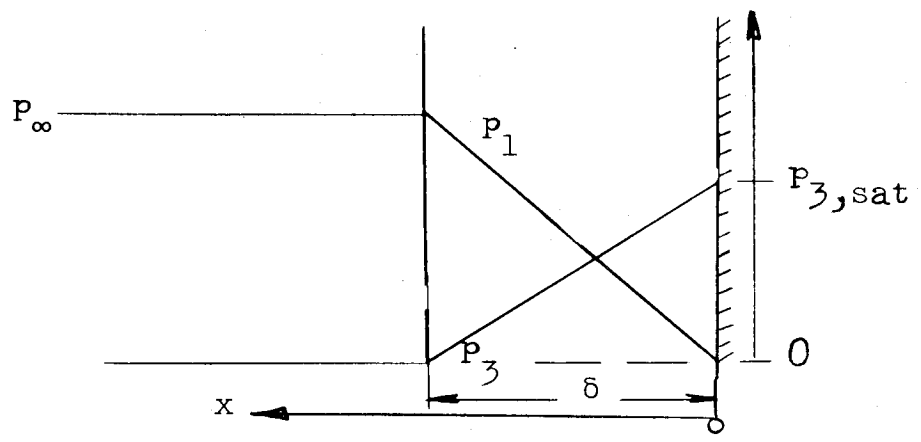

Under the assumptions of simple kinetic theory (ref. 3) the rate of mass diffusion may be written as

$$\frac{dw}{d\theta} = \left[\frac{3m_1}{2\sqrt{2}\pi(\sigma_1 + \sigma_3)^2 p_\infty}\right]\left(\frac{W_1 + W_3}{W_1 W_3} RT\right)^{1/2} \frac{dp_1}{dx} \tag{17}$$

Since the rate of diffusion is constant, the partial pressure of the oxygen is a linear function of x. Then assuming that the partial pressure of the vapor is zero at $x = \delta$ and is saturated at $x = 0$,

$$\frac{dp_1}{dx} = \frac{p_{3,sat}}{\delta} \tag{18}$$

δ will be a function of the external flow field, and if a laminar boundary layer exists, δ will vary approximately inversely as the square root of the free-stream Reynolds number; if free convection persists, δ will vary essentially inversely as the fourth root of the Grashof number and thus will be a function of the difference between the temperatures of the surface and the environment. Thus,

$$\frac{dw}{d\theta} = \frac{\text{Constant}\ \sqrt{N_{Re}}\left(e^{-C/T}\right)\sqrt{T}}{p_\infty} \tag{19}$$

This equation shows the general behavior of the oxidation of metals where the rate of oxidation is controlled by the rate of diffusion of oxygen through oxide vapor. It is seen that oxidation of this nature could lead to ignition and that the rate of oxidation could be markedly increased by subjecting the body to a high-velocity oxygen flow. Should the flow velocity become too great, the control of the oxidation reaction might revert to one of the slower steps in the process. On the other hand, if the body were placed in a quiescent environment at approximately

the surface temperature, the rate of oxidation would become extremely small, and the ignition temperature would be raised considerably.

The case of oxidation controlled by the diffusion of oxygen through a metal vapor film cannot be handled simply. In general, metals of technical importance do not have high vapor pressures, and thus their oxidation rates are not controlled by such a process.

The rate of oxygen transport has been compared with observed oxidation rates at various speeds and altitudes. For this comparison the transport rates were calculated from equation (9) using the partial pressure of oxygen behind a normal shock wave and the stagnation temperature; thus the transport rates are higher than if diffusion through inert gases was considered. The results of these calculations are shown in figure 2. The stagnation temperatures are shown also, and typical metal oxidation rates (for titanium) are added for comparison purposes. Note that at low altitudes the transport rates are several orders of magnitude larger than oxidation rates, and thus transport of this type is definitely not rate controlling under such conditions. At higher altitudes, however, the transport rates are of the same order of magnitude as sea-level oxidation rates, and transport may well be the rate-controlling mechanism. But the transport rate decreases with temperature and thus cannot lead to ignition.

Adsorption of Oxygen Molecules

When an oxygen molecule comes close to the oxide surface it must pass over an "energy hill" if it is to be adsorbed by the surface. Only a small fraction of the molecules coming close to the surface have enough energy to pass this barrier, and thus only a small fraction are adsorbed. Adsorption is believed to occur only at activated sites on the surface. If the pressure of the gaseous reactant is not too low the surface will be covered by a monomolecular layer of adsorbed molecules, and the adsorption is said to be kinetically of zero order.

The rate of zero-order adsorption is given in reference 5 as

$$v = C_a \frac{\kappa T_s}{\hbar} e^{-E/RT_s} \tag{20}$$

where v is the number of molecules adsorbed per unit time, C_a is the number of activated adsorption sites, E is the activation energy representative of the minimum energy a molecule must have to pass over the potential energy barrier, T_s is the surface (and gas) temperature, and κ, $\hbar$, and R are Boltzmann's constant, Planck's constant, and the gas constant, respectively.

The weight rate of adsorption is therefore

$$\frac{dw}{d\theta} = v\,\frac{W_1}{N_o} = C_a\,\frac{\kappa T_s W_1}{N_o \hbar}\,e^{-E/RT_s} \qquad (21)$$

where W_1 is the molecular weight of oxygen, and N_o is Avogadro's number. Note that the rate of adsorption is independent of pressure and is invariant with time. Note also that equation (21) is of the form (over small temperature ranges)

$$\frac{dw}{d\theta} = A_l e^{-E_l/RT_s} \qquad (22)$$

characteristic of metals oxidizing in a linear manner. By comparing the theoretical frequency factor $\left(C_a \kappa T_s W_1/\hbar N_o\right)$ with the experimental constant A_l, some definite conclusions can be drawn concerning the possibility of adsorption as the rate-controlling mechanism for linear oxidation. For the purpose of this comparison C_a is taken as f times number of oxide molecules per unit area, where f is a roughness factor defined by

$$f = \frac{\text{True surface area}}{\text{Projected area}}$$

In the calculations for this comparison f was taken as 25.

Metal	Oxide	T_s, ^oF	$C_a \kappa T_s W_1/\hbar N_o$, g/cm^2-sec	A_l, g/cm^2-sec
Mg	MgO	932	26.4×10^6	1.7×10^6
Ti	TiO_2	1,652	48.5	400
Ca	CaO	932	18.0	.078
U	U_3O_8	572	20.5	7
Ce	CeO_2	572	15.0	.4

Except for magnesium, the theoretical frequency factors are several orders of magnitudes larger than the observed values of A_l, and it does not seem possible that adsorption could be the rate-controlling mechanism. However, the agreement for magnesium is close enough to admit the possibility that adsorption is rate determining for magnesium; in fact, an f of 1.6 would give exact agreement. On the basis of the comparison in the preceding table it can be concluded that adsorption

is one step that may control linear oxidation, but certainly not the only one.

It must be remembered that C_a represents the number of adsorption sites available for oxygen molecules. If the environment is a mixture of oxygen and nonreacting gases, it would seem that some sites would be occupied by the inert molecules. It would be expected, for example, that the number of oxygen adsorption sites in air would be approximately 21 percent of the total number of sites. Thus, if adsorption were indeed the rate-controlling step the oxidation rate would vary directly with the percentage of oxygen in the environment. This behavior might be used to help identify the rate-controlling step for linear oxidation.

If the surface is only sparsely covered with adsorbed molecules, the reaction is said to be kinetically of first order. In this case the rate of adsorption is directly proportional to the oxygen concentration in the environment. It is doubtful that metal oxidations are first order because of the high affinity of oxygen for metals. The first-order reaction, which is considerably more involved than the zero-order adsorption, is discussed in reference 5. Expressions similar to equation (20) may be derived but will not be presented here; it is felt that at the extremely low pressures which are required for first-order reactions the reaction will be limited by the rate of oxygen transport, and adsorption will not be rate controlling.

The adsorption rate predicted by equation (20) is based on the assumption that the gas adsorbed at the surface is essentially at the surface temperature. If, however, the mean free path is of the order of magnitude of the boundary-layer thickness, the molecules which approach the surface may have quite different energies. The higher energy molecules are adsorbed more easily than the colder molecules, and thus any temperature distribution in a thin boundary layer of this type may have a profound influence on the adsorption rate. The activation energy E represents the energy a molecule must have in order to be adsorbed; T_s represents the surface and mean molecular temperature. If the mean temperature of gas molecules is some higher temperature T, then the adsorption rate will be greater by

$$\mathcal{F} = \frac{\text{Fraction of molecules from a group at mean temperature } T \text{ which have energies exceeding } E}{\text{Fraction of molecules from a group at mean temperature } T_s \text{ which have energies exceeding } E}$$

The fraction of molecules from a group at a given temperature which have energies exceeding a given value is (see ref. 3)

$$f_{\text{Energy}>E} = \frac{2}{\sqrt{\pi}}\sqrt{\frac{E}{RT}}\, e^{-E/RT} + 1 - \phi\left(\sqrt{E/RT}\right) \tag{23}$$

where

$$\phi(x) = \frac{2}{\sqrt{\pi}} \int_0^x e^{-x^2} dx$$

It may be shown that for large values of x,

$$1 - \phi(x) \approx \frac{1}{\sqrt{\pi}} \frac{e^{-x^2}}{x}\left(1 - \frac{1}{2x^2} + \ldots\right)$$

Thus, equation (23) is of the form

$$f_{\text{Energy}>E} = \frac{2}{\sqrt{\pi}}\, xe^{-x^2} + \frac{1}{\sqrt{\pi}} \frac{e^{-x^2}}{x}\left(1 - \frac{1}{2x^2} + \ldots\right)$$

where $x^2 = E/RT$. For metals, $10 < E/RT < 50$, and thus, approximately,

$$f_{\text{Energy}>E} \approx \frac{2}{\sqrt{\pi}} \frac{E}{RT}\, e^{-E/RT} \tag{24}$$

Thus,

$$\mathcal{F} \approx \frac{\frac{2}{\sqrt{\pi}}\sqrt{\frac{E}{RT}}\, e^{-E/RT}}{\frac{2}{\sqrt{\pi}}\sqrt{\frac{E}{RT_s}}\, e^{-E/RT_s}} = \frac{1}{\sqrt{(T/T_s)}}\, e^{\frac{E}{RT_s}\left[1 - \frac{1}{(T/T_s)}\right]} \tag{25}$$

The rate of adsorption of molecules whose mean temperature is T by a surface at temperature T_s may therefore be written as

$$\frac{dw}{d\theta} = \left(\frac{dw}{d\theta}\right)_{iso} \cdot \mathcal{F} \approx \left(\frac{dw}{d\theta}\right)_{iso} \sqrt{\frac{T_s}{T}}\, e^{\frac{E}{RT_s}\left[1 - \frac{1}{(T/T_s)}\right]} \tag{26}$$

This analysis may be extended to the situation where there is a temperature variation near the surface. Suppose, for example, that the surface is cool relative to its environment and that a boundary layer of sorts is formed over the surface. The variation of mean molecular temperature away from the surface might be somewhat as shown in the following sketch:

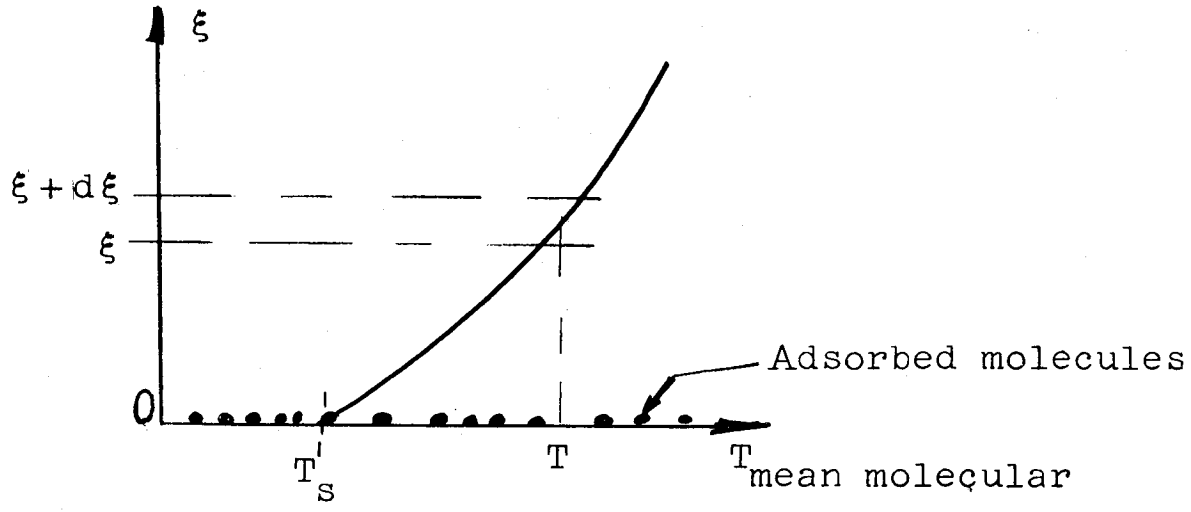

The mean temperature of the molecules in a region between ξ and $\xi + d\xi$ away from the surface is represented by $T(\xi)$. Because of the distribution of molecular free paths, most of the molecules which are adsorbed at the surface come from regions quite close to the surface. The probability that any given adsorbed molecule came from the region $d\xi$ is (ref. 3)

$$P(\xi) = \frac{1}{\lambda_m} e^{-\xi/\lambda_m} d\xi \tag{27}$$

where λ_m is the mean free path. The rate of adsorption of molecules from the interval $d\xi$ is therefore

$$\left(\frac{dw}{d\theta}\right)_{d\xi} = \left(\frac{dw}{d\theta}\right)_{iso} \sqrt{\frac{T_s}{T}}\, e^{\frac{E}{RT_s}\left[1-\frac{T_s}{T(\xi)}\right]} \frac{1}{\lambda_m} e^{-\xi/\lambda_m} d\xi$$

$$= \left(\frac{dw}{d\theta}\right)_{iso} d\mathcal{m} \tag{28}$$

If it is assumed that the temperature distribution does not appreciably influence λ_m, the total rate of adsorption of molecules from all distances is

$$\frac{dw}{d\theta} = \left(\frac{dw}{d\theta}\right)_{iso} \mathcal{m} \tag{29}$$

where

$$m = \int_0^\infty \sqrt{\frac{T_s}{T(\xi)}}\, e^{\frac{E}{RT_s}\left[1-\frac{T_s}{T(\xi)}\right]} e^{-\xi/\lambda_m} d\left(\xi/\lambda_m\right) \qquad (30)$$

The factor m represents the increase in adsorption rate due to the temperature variation away from the surface.

To illustrate the influence of ambient temperature on adsorption rates, equation (30) has been integrated for a linear temperature variation. The results are shown in figure 3. The $a = 0$ situation corresponds to a free molecule flow, and the $a = \infty$ situation represents a thick boundary layer or continuum flow. Note that the ambient temperature can have an appreciable influence in noncontinuum flows, with high temperatures increasing adsorption rates by several orders of magnitude.

Another manner in which high ambient temperatures can influence the rate of adsorption is through dissociation. If the gas surrounding the surface consists of atoms rather than molecules, the mean free path is longer and more higher energy atoms (which originate far from the surface) reach the surface. This effect is compounded by the relative ease with which atoms (compared with molecules) are adsorbed. The result may be a rather substantial increase in the adsorption rate.

Ionization of Oxygen Molecules and Metal Atoms

Very little can be said about the rates of ionization. It is generally believed that ionization rates are much faster than rates of diffusion even through extremely thin films. It would seem that the rates of ionization would not depend upon the thickness of the oxide film and thus would be invariant with time. This means that ionization could not be the rate-controlling step in oxidation that occurs in a time-dependent manner (parabolic oxidation), which indicates that ionization rates are faster than diffusion rates with the possible exception of extremely thin films. Some experiments with ionized gas have been made, and no increase in the reaction rate was observed. Although it cannot be definitely said that ionization rates do not control the linear-type oxidations, it is believed that this is true.

Diffusion of Ions and Electrons

The rate of ion diffusion in oxides has been related to the electrical conductivity by Wagner in reference 6. Electrical charge can be transferred by transfer of ions or electrons which move through the oxide lattice. Most of the metal oxides and nitrides exhibit electronic, as well as ionic, conductivity and are generally classed as semiconductors.

The transference numbers of the cations, anions, and electrons are defined by

$$\tau_A = \frac{l_A}{l_A + l_C + l_e}$$

$$\tau_C = \frac{l_C}{l_A + l_C + l_e}$$

$$\tau_e = \frac{l_e}{l_A + l_C + l_e}$$

where l_C, l_A, and l_e represent portions of the conductivity, or the respective mobilities, of the cation, anion, and electron.

Thus τ_A, τ_C, and τ_e represent the fractions of the electrical conduction due to transfer of cations, anions, and electrons.

If an excess of metal ions (cations) exists, two conduction mechanisms are possible, and they are referred to as "metal excess semiconduction" and "anion deficit semiconduction." In metal excess semiconductors, metal ions and electrons appear interstitially in the lattice, and conduction occurs by migration of cations and electrons. Thus the transference number τ_A is negligible; τ_C is also small, but is of importance. In the anion deficit semiconductor, anions are missing from their respective lattice sites, and electrons are distributed interstitially. Conduction occurs by migration of anions between the defects and electrons in the lattice. Thus τ_C is negligible, and τ_A is small but important. Experimentally it is found that the conductivity of both of these two types of metal excess semiconductors decreases with increased pressure of the negative component (i.e., oxygen). For the first type this is believed to be caused by increased migration of the interstitial cations to new lattice sites at the edge of the crystal, which causes an impoverishment of the interstitial electrons. For the anion deficit semiconductor, an increase in pressure of the negative component causes some of the defects to be filled, reducing the conductivity. Models of these two types of semiconductors are shown as follows:

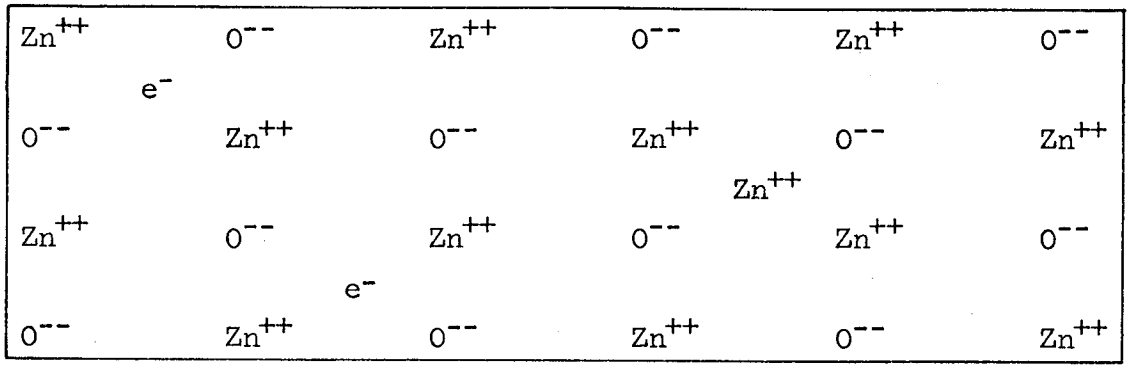

Metal Excess Semiconductor

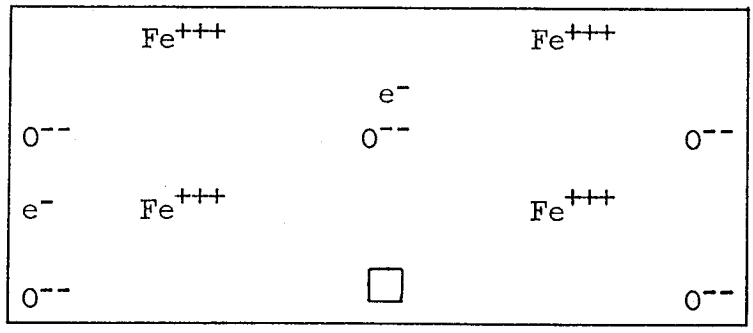

Anion Deficit Semiconductor

If an excess of anions (oxygen ions) exists, two conduction mechanisms are possible, and they are referred to as metal deficit semiconduction and anion excess semiconduction. In metal deficit semiconductors, the cation lattice contains some vacant sites, and electric neutrality is established by the formation of cations of higher valence (termed electron defect). Conduction occurs by electron exchange between cations of different valence and cation migration in the vacant lattice sites. Thus, τ_A is negligible, and τ_C is small but important. In anion excess semiconductors, anions are distributed interstitially, and electric neutrality is maintained by electron defect. Conduction occurs by interchange of electrons between the cations of different valence and anion migration in the interstitial spaces. Thus τ_C is negligible, and τ_A is small but important. It is experimentally found that the conductivity of both of these two types of anion excess semiconductors increases with increased pressure of the negative element (oxygen). For the first type this is said to be due to cation migration to the surface of the crystal leaving more vacant lattice sites and causing more electron defects. For the second type this could be attributed to an increase in the number of interstitial anions, which in turn causes more electron defects. Models for these two types of semiconductors are shown as follows:

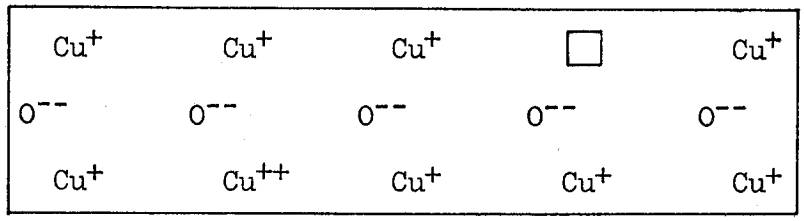

Metal Deficit Semiconductor

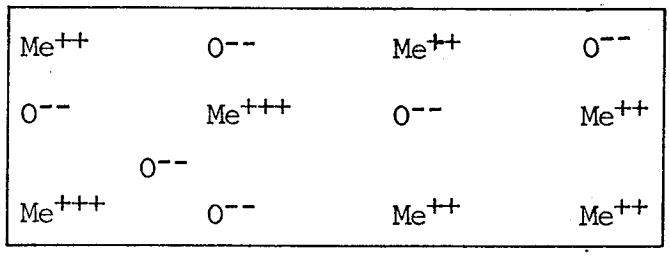

Anion Excess Semiconductor

Wagner, reference 6, has derived an expression for the rate of oxidation in terms of the specific electrical conductivity of the film, the transference numbers of the anions, cations, and electrons, and the free energy decrease of the oxidation reaction. All these quantities can be measured independently, and thus his analysis can be and has been verified experimentally. It is assumed in the analysis that the transport of both ions and electrons through an oxidation layer is fundamentally the same as current flow in a cell. The film provides both the electrolyte by virtue of ionic transport and the external circuit because of electronic conduction. The electromotive force of the cell is assumed to be the decrease in free energy of the reaction. Wagner's analysis leads to

$$\frac{dw}{d\theta} = \frac{z}{\gamma} \frac{(\tau_A + \tau_C)\tau_e}{F\delta} \frac{nRT}{2F^*}\left(p_l^{1/n} - p_m^{1/n}\right) B e^{-E/RT} \qquad (31)$$

Note that this equation has the form, over limited temperature ranges,

$$\frac{dw}{d\theta} = \frac{\text{Constant}}{w} e^{-\text{Constant}/RT} \qquad (32)$$

which in turn leads to an equation of the form

$$w^2 = \text{Constant } e^{-\text{Constant}/RT}\theta = K_p\theta \qquad (33)$$

which is found experimentally to be characteristic of the oxidation of many metals.

It is seen from this analysis that the dependence of the oxidation rate on pressure may be either positive or negative, depending on the semiconduction characteristics of the oxide film. For most metals, this dependence is extremely slight, at least where diffusion is known to be rate controlling. The oxidation rate of copper, for example, varies about as the 1/7 power of the oxygen pressure; the oxidation of zinc varies about as the -1/6 power of pressure.

When an oxygen molecule strikes the surface, it assumes an energy level essentially equivalent to the surface temperature. Ionization and diffusion will then occur at exactly the same rate as if the mean molecular temperature in the gaseous environment were equal to the surface temperature. If dissociation occurs, atoms striking the surface will also assume the surface temperature, and since, in general, atoms are ionized easier than molecules, it might be suspected that the rates of ionization will be faster with dissociation. This is of no consequence since ionization is not important as a rate-controlling step. Thus it appears that the ambient temperature does not influence oxidation where diffusion is the rate-controlling step.

For most metals of technical importance the rate of ion diffusion varies only slightly with pressure. Figure 4 shows the order of magnitude of the influence of flight conditions on diffusion rates for metals where the diffusion rate varies as the $\pm 1/7$ power of (stagnation) pressure. Note that the influence of pressure is relatively small, especially at Mach numbers which would be practical at any altitude. The influence of pressure on the ignition temperature will be slight, with low pressures giving higher ignition temperatures for metals whose oxides are metal deficit semiconductors and lower ignition temperatures for metal excess semiconductors. The mechanism of ion diffusion in the oxide is therefore of importance in determining how ignition temperatures (diffusion controlled) vary with flight conditions.

If the flow over the surface causes the oxide to be blown away, the oxidation will proceed at essentially a constant rate (at any temperature). The partial removal of oxide may increase the rate of diffusion to the point where some other mechanism becomes rate controlling, and thus oxidation data obtained in still air would not apply. This is one of the more important considerations regarding ignition in flight and needs to be studied more carefully.

EXPERIMENTAL RESULTS

The objectives of the experimental part of this investigation were to obtain ignition temperatures for a number of technically important metals and alloys and to support the postulated ignition theory.

Ignition temperatures for a number of metals are presented in table 3. In general, it was observed that the ignition temperatures were relatively independent of the oxygen concentration in the environment; this observation is in agreement with the theories for oxidation controlled by adsorption or diffusion. The ignition temperatures were not appreciably influenced by high-velocity airflow over the oxidizing surface; this indicates either that the airflow was not able to blow away the oxide scale to any appreciable extent or that the removal had little effect on the ignition temperature. The high-velocity airflow should tend to give higher convection coefficients, which should, in turn, lead to higher ignition temperatures according to the theory. However, the increase in the ignition temperatures predicted by the theory is only of the order of 20° to 50° F, and thus it is difficult to determine if there were such an increase. The high-velocity tests therefore neither confirm nor contradict the effect of convection predicted by the theory. The shape of the body seemed to be unimportant, at least in the range of conditions obtainable. Thus, the use of an isothermal body as a basis for analysis may not be too bad, except under more extreme circumstances.

In general, the experimental observations and the theory of ignition are in reasonable agreement, and the behavior of actual ignition temperatures with environmental conditions is predicted quite adequately by the theory.

Apparatus and Procedures

The experimental part of this investigation consisted of three phases. In the first phase several metals were heated electrically in a specially constructed container in which controlled environments could be maintained. The temperature of the samples was raised until ignition or melting occurred, and the failure temperature was measured with an optical pyrometer. In the second phase metals were heated electrically in a jet of air at a Mach number of 1.25, and failure temperatures were observed optically. In the third phase calcium models of various shapes were placed in a hot airstream, and ignition temperatures were measured with thermocouple circuits.

The pressure tank and control console used in the first phase are shown in figures 5 and 6. The models were strips or wires of various dimensions and were abraded prior to testing to remove all oxide scale. Air or oxygen pressures of up to 8 atmospheres could be maintained in the tank. A quartz window and mirror train allowed observation with the optical pyrometer. The temperature at which the model temperature started to increase rapidly was recorded as the ignition temperature; in some cases the models simply melted, and the observed melting point was recorded. The observed temperatures were corrected for adsorption

by the window and mirror train but were not corrected for the fact that the target was not a true black body. The temperatures reported are therefore "brightness" temperatures and are lower than the true temperatures. In each case the uncertainty in temperature was estimated and recorded.

The free-jet wind-tunnel installation used in the second phase is shown in figure 7. The discharge area is 0.760 square inch, and stagnation temperatures up to 180° F may be obtained. A typical model is shown suspended between the electrodes. The technique for measuring the ignition temperatures was the same as that used in the pressure tank, except that no correction for a mirror train was required.

The high-temperature-air supply used in the third phase is shown in figure 8. Air was heated electrically by a series of Nichrome screens, and temperatures up to 1,850° F at 100 ft/sec could be obtained. The discharge area was 1 square inch. The models were calcium cones of various shapes with iron-constantan thermocouples mounted in the tips. Immediately prior to testing, the models were abraded to remove the oxide scale, and the points were sharpened. The air temperature was then increased slowly, and the model temperature recorded on a fast response millivoltmeter. When ignition occurred the model temperature rose rapidly, and the ignition temperature was well defined by a sharp break in the temperature-time curve.

Test Results

The experiments in the pressure tank were performed to determine the effect of the environmental pressure on the ignition temperature. In no case was any appreciable effect observed, and this is in agreement with the mechanisms and thermal definition of ignition. The observed melting points are in agreement with the well-known values. There is some scatter in the data, and this may be due to time dependencies of the oxidation rate, although effort was made to have the warmup time of all models the same. Models of various thicknesses were tested, and no effect of thickness was observed. Since the rate of burning after ignition was considerably greater with oxygen than with air, the ignition temperature was better defined with oxygen, and thus the data obtained using oxygen are probably more accurate. No appreciable difference between the ignition temperatures in air and oxygen was observed, which indicates that diffusion in the oxide controlled the reaction.

The experiments in the supersonic jet were performed to study the effect of flow velocity. It was expected that the thickness of the oxide film might be reduced by the flow, thus lowering the ignition temperature. No appreciable effect of the jet was observed.

Unfortunately, the convection conductances were not high enough so that the effect of convection heat transfer predicted by the analysis could be checked.

The experiments in the hot airstream were performed to study the effect of shape. Calcium was chosen as the test metal because it has an ignition temperature in the range of the temperatures producible in the jet, because it is known to oxidize in a time-independent manner, and because it has reasonably good strength characteristics in the range of ignition. Magnesium was tried at first, but the models sagged before ignition and thus were useless for a study of the shape effect. Cones having included angles of from 20° to 180° and base diameters of 3/8 inch were tested at approximately 85 ft/sec, and no appreciable effect of shape was observed. Ignition was seen to occur first at the very tip of the models and then to propagate to the afterbody. In a few seconds the entire model was consumed. The possibility of a shape effect cannot be ruled out entirely, because it is probable that the shape effect will be more pronounced at more rapid heating rates.

Table 3 presents a summary of ignition temperatures of solid metals obtained under static conditions. The data of a number of other investigators are included. The results of the pressure tank and supersonic wind-tunnel tests of this investigation are presented in tables 4 to 23 and in figures 9 to 17. The results of the shape-effect experiments are presented in table 24.

Comparison of Predicted and Experimental Ignition Temperatures

The experimental ignition temperatures for a number of metals are compared with the ignition temperatures predicted by the thermal definition of ignition in figure 18. In this comparison the oxidation data of table 1 and the heats of formation of table 25 were used. In addition, the comparison is made for several magnesium alloys. The oxidation data for these comparisons for magnesium were taken from reference 7 and the ignition-temperature data were taken from reference 8, and both are summarized in table 26.

In figure 18 the experimental data are compared with the curve for $h^* = 0$; this is reasonable for a qualitative comparison, since the ignition temperatures were all measured in quiescent environments. It must be remembered that the uncertainty in the oxidation rate constants is extremely high and thus the comparison cannot be too quantitative. It is felt that the agreement of the data with the theoretical ignition temperatures is satisfactory, and thus the postulate of a direct relation between oxidation and ignition, and all consequences thereof, is correct.

CONCLUDING REMARKS

A simplified definition of ignition has been developed from an energy balance on an isothermal body. The conclusions regarding the effects of environmental factors on the ignition temperature are thus restricted to situations where internal temperature gradients are relatively small, but more drastic shapes may well produce substantial departures from the predicted behavior. The simple analysis, and consideration of the oxidation mechanisms, indicate that the ignition temperature is essentially independent of ambient temperature and pressure, except insofar as these items influence convective heat transfer. The dependence of the ignition temperature on convection and radiation heat-transfer rate predicted by the analysis is extremely interesting. It is found that the ignition temperature depends only on the magnitude of these transfers and not upon their direction, with higher heating or cooling rates giving higher ignition temperatures. No data are available either to substantiate or to repudiate this result. Under certain circumstances the ignition temperature depends on the thickness of the oxide scale covering the surface, and thus any factors which might tend to reduce the scale thickness are important. The available data are in reasonably good agreement with the postulated mechanisms and the thermal definition of ignition.

Stanford University,
Stanford, Calif., June 15, 1957.

REFERENCES

1. Hill, Paul R., Adamson, David, Foland, Douglas H., and Bressette, Walter E.: High-Temperature Oxidation and Ignition of Metals. NACA RM L55L23b, 1956.

2. Kubaschewski, O., and Hopkins, B. E.: Oxidation of Metals and Alloys. Butterworths Sci. Pub. (London), 1953.

3. Kennard, Earle H.: Kinetic Theory of Gases. McGraw-Hill Book Co, Inc., 1938.

4. Hodgman, Charles D., ed.: Handbook of Chemistry and Physics. Thirty-six ed., Chemical Rubber Pub. Co., 1954-1955.

5. Glasstone, Samuel, Laidler, Keith J., and Eyring, Henry: The Theory of Rate Processes. First ed., McGraw-Hill Book Co., Inc., 1941.

6. Wagner, C.: Bietrag zur Theorie des Anlaufvorgangs. Zeitschr. f. phys. Chem., Abt. B, Bd. 21, July 1933, pp. 25-41.

7. Leontis, T. E., and Rhines, F. N.: Rates of High-Temperature Oxidation of Magnesium and Magnesium Alloys. Tech. Pub. No. 2003, Am. Inst. Mining and Metallurgical Eng., Feb. 1946.

8. Fassell, W. Martin, Jr., Gulbransen, Leonard B., Lewis, John R., and Hamilton, J. Hugh: Ignition Temperatures of Magnesium and Magnesium Alloys. Jour. Metals, vol. 3, no. 7, July 1951, pp. 522-528.

9. Conway, J. B., and Kirshenbaum, M. S.: Ninth Progress Report. Contract N9-ONR-87301, Res. Inst. of Temple Univ., Jan. 1, 1954.

10. Loriers, Jean: Sur l'oxydation de l'uranium métallique. Comptes Rendus, t. 234, no. 1, Jan. 2, 1952, pp. 91-93.

11. Loriers, Jean: Sur l'oxydation du cérium et du lanthane. Comptes Rendus, t. 229, no. 11, Sept. 12, 1949, pp. 547-549.

TABLE 1

OXIDATION DATA FOR METALS

Metal	Primary oxide	Gas	Pressure, mm. Hg	Temperature range, °F	A_p, g^2/cm^4-sec	A_l, g/cm^2-sec	E_p or E_l, cal/mole
Be	BeO	O_2	100	840 to 970	0.22	---	62,000
	BeO	O_2	76	350 to 700	1.8×10^{-12}	---	8,500
	BeO	O_2	76	750 to 950	3.5×10^{-3}	---	50,300
Mg	MgO	O_2	760	475 to 575	---	1.7×10^{6}	50,500
Ca	CaO	O_2	760	600	---	.2	19,600
Th	ThO_2	O_2	450	250 to 350	.073	---	31,000
	ThO_2	O_2	210	350 to 450	---	.078	22,000
	ThO_2	O_2	210	450	---	10.9	25,600
Ti	Rutile	O_2	76	400 to 600	2.0×10^{-5}	---	29,300
	Rutile	O_2	760	650 to 830	---	400	40,000
	Rutile	O_2	760	830 to 950	---	5	47,000
Zr	ZrO_2	O_2	76	200 to 425	2.9×10^{-7}	---	18,200
	ZrO_2	O_2	74	600 to 920	2.4×10^{-3}	---	32,000
V	V_2O_5	O_2	76	400 to 600	1.3×10^{-3}	---	30,700
Nb	NbO	O_2	76	200 to 375	2.6×10^{-5}	---	27,400
Ta	Ta_2O_5	O_2	76	250 to 450	3.5×10^{-4}	---	27,400
		O_2	760	1,250	65	---	43,700
Cr	Cr_2O_3	O_2	76	700 to 900	31.5	---	66,300
Mo	MoO_3	O_2	76	350 to 450	3.55×10^{-2}	---	36,500
W	WO_3	O_2	76	400 to 840	5.1×10^{3}	---	54,000
Mn	Mn_3O_4	Air		400 to 1,000	1.95×10^{-3}	---	28,300
Fe	FeO	Air		500 to 1,100	.37	---	33,000
Co	CoO	O_2	76	200 to 400	2.0×10^{-5}	---	23,400
		O_2	76	300 to 600	3.0×10^{-6}	---	22,200
		Air		400 to 625	3.0×10^{-6}	---	22,200
Ni	NiO	Air		625 to 1,100	.56	---	44,100
		Air		750 to 1,240	3.2×10^{-2}	---	45,000
Cu	Cu_2O	Air		300 to 550	1.5×10^{-5}	---	20,140
	CuO	Air		550 to 900	.266	---	37,700
Al	Al_2O_3	O_2	76	350 to 475	$2 - 7.5 \times 10^{-8}$	---	22,800
Pb	PbO	Air		100 to 300	.009	---	24,200
Ce	Ce_2O_3, CeO_2	Air	760	300	---	.4	7,000
U	U_3O_8			300	---	7	18,400

TABLE 2

SUMMARY OF POSSIBLE OXIDATION-RATE-CONTROLLING MECHANISMS

SHOWING THE INFLUENCE OF ENVIRONMENTAL FACTORS

Mechanism	Simplified rate formula	Remarks
Transport mechanisms:		
Molecular collision in pure oxygen	$\frac{dw}{d\theta} = \text{Constant}\ \ p/\sqrt{T}$	Will not lead to ignition
Oxygen diffusion through nonreacting gas	[a] $\frac{dw}{d\theta} = \text{Constant}\ \ \frac{p_\infty}{p_1}\sqrt{T}\sqrt{N_{Re}}$	Will not lead to ignition; may depend somewhat on T_∞
Oxygen diffusion through oxide vapor	[a] $\frac{dw}{d\theta} = \text{Constant}\ \ \frac{\sqrt{T}}{p_\infty}\sqrt{N_{Re}}\ e^{-C/T}$	May depend somewhat on T_∞; known to be rate controlling for molybdenum
Reaction in metal vapor film		Extremely rapid reaction, but not common in technically important metals below the ignition temperature
Adsorption of oxygen at gas-oxide interface	$\frac{dw}{d\theta} = \text{Constant}\ \ \frac{p_{O_2}}{p_\infty}\ Te^{-E/RT}$	Believed to be rate controlling for magnesium; independent of flow velocity
Ionization of oxygen and metal		Not believed to be rate controlling for metals
Diffusion mechanisms:		
Cation excess semiconductors	$\frac{dw}{d\theta} = \frac{\text{Constant}}{\delta}\left(p_{O_2}\right)^{-1/n_e}e^{-E/RT}$	Usually only slightly decreasing with oxygen pressure; independent of flow velocity (example: ZnO)
Anion excess semiconductors	$\frac{dw}{d\theta} = \frac{\text{Constant}}{\delta}\left(p_{O_2}\right)^{1/n_e}e^{-E/RT}$	Usually only slightly increasing with oxygen pressure; independent of flow velocity (example: Cu_2O)

[a] Below some limit the oxidation rate will be independent of Reynolds number; $\sqrt{N_{Re}}$ holds for the laminar boundary layer.

TABLE 3

IGNITION TEMPERATURES OF SOLID METALS

Metal	Ignition temperature, °F	Source	Gas	Pressure, atm
Mild steel	2,240 to [a]2,330	(b)	Air,(c)	1 to 7
W	2,270 to [a]2,350	(b)	Air,(c)	1 to 7
Ta	2,260 to [a]2,340	(b)	Air,(c)	1 to 7
Ti alloys:				
RC-70	2,880 to [a]2,960	(b)	Air,O_2	1 to 7
RS-70	2,890 to [a]2,940	(b)	Air,O_2	1 to 7
RS-110-A	2,860 to [a]2,910	(b)	(d),O_2	1 to 7
RS-110-BX	2,850 to [a]2,920	(b)	(d),O_2	1 to 7
Stainless steels:				
430	2,460 to [a]2,490	(b)	(d),O_2	1 to 7
302	(e)	(b)	Air,O_2	1 to 7
Cu	(e)	(b)	Air,O_2	1 to 7
Ni	(e)	(b)	Air,O_2	1 to 7
Ni alloys:				
Inconel	(e)	(b)	Air,O_2	1 to 7
Inconel X	(e)	(b)	Air,O_2	1 to 7
Be alloys:				
Berylco 10	1,750 to 1,760	(b)	Air,O_2	1 to 7
Berylco 25	(e)	(b)	Air,O_2	1 to 7
Mg	1,171	ref. 6	O_2	1 to 10
Mg alloys:				
20% Al	936	ref. 7	O_2	1
70% Zn	1,004	ref. 7	O_2	1
25% Ni	934	ref. 7	O_2	1
20% Sb	1,099	ref. 7	O_2	1
63% Al	862	ref. 7	O_2	1
Fe	1,706	ref. 9	O_2	1
Sr	1,328	ref. 9	O_2	1
Ca	1,022	ref. 9	O_2	1
Th	932	ref. 9	O_2	1
Ba	347	ref. 9	O_2	1
Mo	1,400	ref. 9	O_2	1
U	608	ref. 10	O_2	1
Ce	608	ref. 11	O_2	1
Al	(e)	ref. 9	O_2	1
Zn	(e)	ref. 9	O_2	1
Pb	(e)	ref. 9	O_2	1
Sn	(e)	ref. 9	O_2	1
Bi	(e)	ref. 9	O_2	1
Li	(e)	ref. 9	O_2	1
Cd	(e)	ref. 9	O_2	1
Na	(e)	ref. 9	O_2	1
K	(e)	ref. 9	O_2	1

[a]Brightness temperature.

[b]Present investigation.

[c]Not tested in oxygen, but probably ignites in oxygen at about the same temperature.

[d]Does not ignite in air.

[e]Melts before igniting.

TABLE 4

TANK TESTS WITH MILD STEEL

Run	Model specifications		Gas	Pressure, atm	Ambient temperature, °F	Humidity, $\frac{\text{lb } H_2O}{\text{lb air}}$	Power at failure, w	Brightness ignition temperature, °F
	Length, in.	Diameter, in.						
1	2	0.080	Air	1	74	0.006	[a]160	2,330 ± 20
2	2	.080	Air	1	74	.006	----	2,320 ± 20
3	2	.080	Air	1	74	.006	----	2,240 ± 20
4	2	.080	Air	1	74	.006	----	2,280 ± 20
5	2	.080	Air	1	75	.006	----	2,260 ± 20
6	2	.080	Air	2	75	.006	----	2,340 ± 20
7	2	.080	Air	2	75	.006	----	2,280 ± 20
8	2	.080	Air	2	72	.006	----	2,330 ± 20
9	2	.080	Air	2	76	.006	----	2,380 ± 20
10	2	.080	Air	2	76	.006	----	2,330 ± 20
11	2	.080	Air	3	77	.006	----	2,310 ± 20
12	2	.080	Air	3	77	.006	----	2,280 ± 20
13	2	.080	Air	3	77	.006	----	2,290 ± 20
14	2	.080	Air	3	77	.006	----	2,300 ± 20
15	2	.080	Air	5	78	.006	----	2,330 ± 20
16	2	.080	Air	5	78	.006	----	2,280 ± 20
17	2	.080	Air	5	79	.006	----	2,320 ± 20
18	2	.080	Air	8	79	.006	----	2,300 ± 20
19	2	.080	Air	8	78	.006	----	2,320 ± 20
20	2	.080	Air	8	78	.006	----	2,310 ± 20

[a]Nominal.

TABLE 5

TANK TESTS WITH TUNGSTEN

Run	Model specifications		Gas	Pressure, atm	Ambient temperature, °F	Humidity, lb H_2O / lb air	Power at failure, w	Brightness ignition temperature, °F
	Length, in.	Diameter, in.						
1	2	0.036	Air	1	74	0.006	[a]60	2,340 ± 20
2	2	.036	Air	1	74	.006	---	2,350 ± 20
3	2	.036	Air	2	74	.006	---	2,300 ± 20
4	2	.036	Air	2	74	.006	---	2,280 ± 20
5	2	.036	Air	3	74	.006	---	2,280 ± 20
6	2	.036	Air	3	74	.006	---	2,270 ± 20
7	2	.036	Air	4	74	.006	---	2,370 ± 20
8	2	.036	Air	5	74	.006	---	2,340 ± 20
9	2	.036	Air	5	74	.006	---	2,370 ± 20
10	2	.036	Air	6	74	.006	---	2,280 ± 20
11	2	.036	Air	6	74	.006	---	2,340 ± 20
12	2	.036	Air	7	74	.006	---	2,340 ± 20
13	2	.036	Air	7	74	.006	---	2,300 ± 20

[a]Nominal.

TABLE 6

TANK TESTS WITH TANTALUM

Run	Model specifications			Gas	Pressure, atm	Ambient temperature, °F	Humidity, lb H_2O / lb air	Power at failure, w	Brightness ignition temperature, °F
	Length, in.	Width, in.	Thickness, in.						
1	1	1/4	0.02	Air	1	74	0.006	[a]100	2,300 ± 20
2	1	1/4	.02	Air	1	74	.006	----	2,260 ± 20
3	1	1/4	.02	Air	2	74	.006	----	2,330 ± 20
4	1	1/4	.02	Air	2	74	.006	----	2,310 ± 20
5	1	1/4	.02	Air	3	74	.006	----	2,320 ± 20
6	1	1/4	.02	Air	3	74	.006	----	2,260 ± 20
7	1	1/4	.02	Air	4	74	.006	----	2,340 ± 20
8	1	1/4	.02	Air	4	74	.006	----	2,340 ± 20
9	1	1/4	.02	Air	4	74	.006	----	2,300 ± 20
10	1	1/4	.02	Air	4	74	.006	----	2,310 ± 20
11	1	1/4	.02	Air	5	74	.006	----	2,280 ± 20
12	1	1/4	.02	Air	5	74	.006	----	2,300 ± 20
13	1	1/4	.02	Air	6	74	.006	----	2,320 ± 20
14	1	1/4	.02	Air	6	74	.006	----	2,280 ± 20
15	1	1/4	.02	Air	7	74	.006	----	2,290 ± 20
16	1	1/4	.02	Air	7	74	.006	----	2,290 ± 20
17	1	1/4	.02	Air	8	74	.006	----	2,320 ± 20
18	1	1/4	.02	Air	8	74	.006	----	2,330 ± 20

[a]Nominal.

TABLE 7

TANK TESTS WITH TITANIUM RC-70

Run	Model specifications			Gas	Pressure, atm	Ambient temperature, °F	Humidity, $\frac{\text{lb } H_2O}{\text{lb air}}$	Power at failure, w	Brightness ignition temperature, °F
	Length, in.	Width, in.	Thickness, in.						
1	1.5	1/8	0.020	O_2	1	70	------	101	2,930 ± 30
2	1.5	1/8	.020	O_2	1	70	------	114	2,880 ± 30
3	1.5	1/4	.067	O_2	2	70	------	1,150	2,940 ± 30
4	1.5	1/8	.067	O_2	3	70	------	460	2,910 ± 20
5	1.5	1/8	.040	O_2	4	70	------	295	2,890 ± 20
6	1.5	1/8	.040	O_2	4	70	------	300	2,930 ± 20
7	1.5	1/4	.067	O_2	5	70	------	1,220	2,930 ± 20
8	1.5	1/8	.010	O_2	6	70	------	-----	2,895 ± 20
9	1.25	1/4	.067	O_2	7	70	------	840	2,900 ± 30
10	1.5	1/4	.067	O_2	7	70	------	940	2,880 ± 30
11	1.5	1/4	.010	Air	1	63	0.0080	-----	2,910 ± 20
12	1.5	1/4	.010	Air	2	63	.0080	-----	2,900 ± 30
13	1.5	1/4	.010	Air	3	63	.0080	-----	2,910 ± 20
14	1.5	1/4	.010	Air	4	63	.0080	-----	2,890 ± 30
15	1.5	1/4	.010	Air	5	63	.0080	-----	2,920 ± 20
16	1.5	1/4	.010	Air	6	63	.0080	-----	2,940 ± 20
17	1.5	1/4	.010	Air	7	63	.0080	-----	2,920 ± 20
18	1.5	1/4	.067	He	1	63	------	-----	[a]3,010 ± 20

[a]Melted.

TABLE 8

WIND-TUNNEL TEST OF TITANIUM RC-70

Run	Model specifications			Mach number	Humidity of jet, $\frac{\text{lb } H_2O}{\text{lb dry air}}$	Stagnation temperature, °F	Power at failure, w	Brightness ignition temperature, °F
	Length, in.	Width, in.	Thickness, in.					
1	1.88	0.138	0.067	1.25	0.00184	163	1,670	2,950 ± 10
2	1.88	.202	.067	1.25	.00184	197	1,800	2,880 ± 20
3	1.88	.237	.067	1.25	.00184	163	2,210	2,950 ± 20
4	1.88	.237	.067	1.25	.00184	140	1,900	2,960 ± 20

TABLE 9

TANK TESTS WITH TITANIUM RS-70

Run	Model specifications			Gas	Pressure, atm	Ambient temperature, °F	Humidity, lb h_2O / lb dry air	Power at failure, w	Brightness ignition temperature, °F
	Length, in.	Width, in.	Thickness, in.						
1	1.5	3/16	0.025	O_2	1	71	------	311	2,920 ± 20
2	1.5	3/16	.025	O_2	3	71	------	281	2,940 ± 10
3	1.5	3/16	.025	O_2	4	71	------	307	2,920 ± 20
4	1.5	3/16	.025	O_2	5	71	------	285	2,940 ± 10
5	1.5	3/16	.025	O_2	6	71	------	307	2,930 ± 20
6	1.5	3/16	.025	O_2	7	71	------	281	2,890 ± 20
7	1.5	3/16	.025	Air	1	73	0.0062	298	2,930 ± 30
8	1.5	3/16	.025	Air	1	73	.0062	304	2,970 ± 30
9	1.5	3/16	.025	Air	1	73	.0062	298	3,000 ± 30
10	1.5	3/16	.025	Air	3	73	.0062	298	3,010 ± 30
11	1.5	3/16	.025	Air	5	73	.0062	298	2,930 ± 30
12	1.5	3/16	.025	Air	7	73	.0062	310	2,960 ± 30

TABLE 10

WIND-TUNNEL TESTS OF TITANIUM RS-70

Run	Model specifications			Mach number	Humidity of jet, $\frac{\text{lb } H_2O}{\text{lb dry air}}$	Stagnation temperature, °F	Brightness ignition temperature, °F
	Length, in.	Width, in.	Thickness, in.				
1	1.88	0.188	0.025	1.25	0.00184	105	2,950 ± 30
2	1.88	.188	.025	1.25	.00184	105	2,940 ± 30

TABLE 11

TANK TESTS WITH TITANIUM RS-110-A

Run	Model specifications			Gas	Pressure, atm	Ambient temperature, °F	Humidity, lb H_2O / lb dry air	Power at failure, w	Brightness ignition temperature, °F
	Length, in.	Width, in.	Thickness, in.						
1	1.5	3/16	0.025	O_2	1	71	------	282	2,890 ± 20
2	1.5	3/16	.025	O_2	3	71	------	300	2,890 ± 30
3	1.5	3/16	.025	O_2	5	71	------	331	2,890 ± 10
4	1.5	3/16	.025	O_2	7	71	------	328	2,910 ± 20
5	1.5	3/16	.025	O_2	8	71	------	307	2,860 ± 20
6	1.5	3/16	.025	Air	1	73	0.0081	288	[a]3,260 ± 100
7	1.5	3/16	.025	Air	1	73	.0081	260	[a]3,260 ± 50
8	1.5	3/16	.025	Air	3	73	.0081	325	[a]3,110 ± 50
9	1.5	3/16	.025	He	1	70	------	330	[a]3,040 ± 50

[a]Melted.

TABLE 12

WIND-TUNNEL TESTS OF TITANIUM RS-110-A

Run	Model specifications			Mach number	Humidity of jet, $\frac{\text{lb } H_2O}{\text{lb dry air}}$	Stagnation temperature, ^{o}F	Brightness ignition temperature, ^{o}F
	Length, in.	Width, in.	Thickness, in.				
1	1.88	0.188	0.025	1.25	0.00184	140	[a]2,760 ± 30
2	1.88	.188	.025	1.25	.00184	140	[a]2,720 ± 30
3	1.88	.188	.010	1.25	.00184	140	[a]3,040 ± 30
4	1.88	.188	.010	1.25	.00184	140	[a]3,060 ± 30

[a]Melted.

TABLE 13

TANK TESTS WITH TITANIUM RS-110-BX

Run	Model specifications			Gas	Pressure, atm	Ambient temperature, °F	Humidity, lb H_2O / lb dry air	Power at failure, w	Brightness ignition temperature, °F
	Length, in.	Width, in.	Thickness, in.						
1	1.5	3/16	0.025	O_2	1	70	------	248	2,910 ± 20
2	1.5	3/16	.025	O_2	1	70	------	260	2,850 ± 20
3	1.5	3/16	.025	O_2	3	70	------	272	2,920 ± 20
4	1.5	3/16	.025	O_2	5	70	------	265	2,900 ± 20
5	1.5	3/16	.025	O_2	7	70	------	282	2,890 ± 20
6	1.5	3/16	.025	O_2	8	70	------	300	2,890 ± 20
7	1.5	3/16	.025	Air	1	70	0.0075	264	[a]3,280 ± 50
8	1.5	3/16	.025	Air	1	68	------	---	[a]3,150 ± 30
9	1.5	3/16	.025	Air	1	68	------	---	[a]3,040 ± 30
10	1.5	3/16	.025	Air	5	70	.0075	306	[a]3,050 ± 50
11	1.5	3/16	.025	Air	8	70	.0075	278	[a]3,270 ± 50

[a]Melted.

TABLE 14

WIND-TUNNEL TESTS OF TITANIUM RS-110-BX

Run	Model specifications			Mach number	Humidity of jet, $\frac{\text{lb } H_2O}{\text{lb dry air}}$	Stagnation temperature, $^{\circ}F$	Brightness ignition temperature, $^{\circ}F$
	Length, in.	Width, in.	Thickness, in.				
1	1.88	0.188	0.025	1.25	0.00184	140	2,940 ± 20
2	1.88	.188	.025	1.25	.00184	140	2,880 ± 20
3	1.88	.188	.025	1.25	.00184	140	2,830 ± 20
4	1.88	.188	.025	1.26	.00184	140	2,850 ± 20
5	1.88	.188	.025	1.25	.00184	140	3,050 ± 20
6	1.88	.188	.010	1.25	.00184	140	2,930 ± 20
7	1.88	.188	.010	1.25	.00184	140	2,910 ± 20
8	1.88	.188	.010	1.25	.00184	140	2,950 ± 20
9	1.88	.188	.010	1.25	.00184	140	2,950 ± 20
10	1.88	.188	.010	1.25	.00184	140	2,930 ± 20

TABLE 15

TANK TESTS WITH STAINLESS STEEL 430

Run	Model specifications			Gas	Pressure, atm	Ambient temperature, °F	Humidity, lb H_2O / lb dry air	Power at failure, w	Brightness ignition temperature, °F
	Length, in.	Width, in.	Thickness, in.						
1	1.75	3/16	0.025	O_2	1	67	------	243	2,470 ± 20
2	1.75	3/16	.025	O_2	1	67	------	233	2,490 ± 20
3	1.75	3/16	.025	O_2	3	67	------	223	2,480 ± 20
4	1.75	3/16	.025	O_2	5	67	------	205	2,460 ± 20
5	1.75	3/16	.025	O_2	5	67	------	205	2,470 ± 20
6	1.75	3/16	.010	O_2	7	67	------	---	2,480 ± 20
7	1.75	3/16	.025	Air	1	67	0.0065	261	[a]2,670 ± 30
8	1.75	3/16	.025	Air	1	67	.0065	284	[a]2,680 ± 30
9	1.75	3/16	.025	Air	4	67	.0065	244	[a]2,710 ± 30
10	1.75	3/16	.025	Air	7	67	.0065	294	[a]2,720 ± 30

[a]Melted.

TABLE 16

WIND-TUNNEL TEST OF STAINLESS STEEL 430

Run	Model specifications			Mach number	Humidity of jet, lb H_2O / lb dry air	Stagnation temperature, °F	Brightness ignition temperature, °F (a)
	Length, in.	Width, in.	Thickness, in.				
1	1.88	0.188	0.025	1.25	0.00184	110	2,730 ± 20
2	1.88	.188	.025	1.25	.00184	107	2,780 ± 40

[a]Model melted.

TABLE 17

TANK TESTS WITH STAINLESS STEEL 302

Run	Model specifications			Gas	Pressure, atm	Ambient temperature, °F	Humidity, lb H_2O / lb dry air	Power at failure, w	Brightness ignition temperature, °F (a)
	Length, in.	Width, in.	Thickness, in.						
1	1.5	3/16	0.025	O_2	1	71	------	254	2,600 ± 30
2	1.5	3/16	.025	O_2	1	71	------	259	2,550 ± 30
3	1.5	3/16	.025	O_2	3	71	------	255	2,500 ± 20
4	1.5	3/16	.025	O_2	5	71	------	266	2,520 ± 20
5	1.5	3/16	.025	O_2	7	71	------	255	2,520 ± 20
6	1.5	3/16	.025	O_2	8	71	------	247	2,510 ± 20
7	1.5	3/16	.025	Air	1	71	0.0050	292	2,550 ± 20
8	1.5	3/16	.025	Air	1	71	.0050	320	2,510 ± 20
9	1.5	3/16	.025	Air	3	71	.0050	296	2,550 ± 20
10	1.5	3/16	.025	Air	5	71	.0050	289	2,540 ± 20
11	1.5	3/16	.025	Air	8	71	.0050	310	2,590 ± 20

[a]Model melted.

TABLE 18

TANK TESTS WITH COPPER

Run	Model specifications		Gas	Pressure, atm	Ambient temperature, °F	Humidity, lb H_2O / lb dry air	Power at failure, w	Brightness ignition temperature, °F (a)
	Length, in.	Diameter, in.						
1	1.75	0.020	O_2	1	63	------	27.3	1,880 ± 20
2	1.75	.020	O_2	1	63	------	25.4	1,860 ± 20
3	1.75	.020	O_2	2	63	------	27.3	1,870 ± 10
4	1.75	.020	O_2	4	63	------	25.3	1,865 ± 10
5	1.75	.020	O_2	6	63	------	27.3	1,860 ± 20
6	1.75	.020	O_2	8	63	------	28.3	1,860 ± 20
7	1.75	.020	Air	1	63	0.0086	27.3	1,865 ± 10
8	1.75	.020	Air	2	63	.0086	27.3	1,880 ± 20
9	1.75	.020	Air	4	63	.0086	28.3	1,860 ± 10
10	1.75	.020	Air	6	63	.0086	26.1	1,880 ± 20
11	1.75	.020	Air	8	63	.0086	26.3	1,850 ± 20
12	1.75	.020	He	1	71	------	----	1,830 ± 15

[a]Model melted.

TABLE 19

TANK TESTS WITH NICKEL

Run	Model specifications			Gas	Pressure, atm	Ambient temperature, °F	Humidity, lb H_2O / lb dry air	Power at failure, w	Brightness ignition temperature, °F (a)
	Length, in.	Width, in.	Thickness, in.						
1	1.5	3/16	0.025	O_2	1	71	------	234	2,540 ± 20
2	1.5	3/16	.025	O_2	3	71	------	246	2,550 ± 20
3	1.5	3/16	.025	O_2	5	71	------	234	2,545 ± 20
4	1.5	3/16	.025	O_2	7	71	------	256	2,545 ± 20
5	1.5	3/16	.025	O_2	8	71	------	250	2,550 ± 20
6	1.5	3/16	.025	Air	1	71	0.0050	226	2,540 ± 20
7	1.5	3/16	.025	Air	4	71	.0050	252	2,550 ± 20
8	1.5	3/16	.025	Air	6	71	.0050	250	2,540 ± 20
9	1.5	3/16	.025	He	1	71	------	---	2,400 ± 15

[a]Model melted.

TABLE 20

TANK TESTS WITH INCONEL

Run	Model specifications			Gas	Pressure, atm	Ambient temperature, °F	Humidity, lb H_2O / lb dry air	Power at failure, w	Brightness ignition temperature, °F (a)
	Length, in.	Width, in.	Thickness, in.						
1	1.5	3/16	0.018	O_2	1	69	------	281	2,550 ± 20
2	1.5	3/16	.018	O_2	1	69	------	268	2,520 ± 20
3	1.5	3/16	.018	O_2	3	69	------	281	2,520 ± 20
4	1.5	3/16	.018	O_2	5	69	------	297	2,550 ± 20
5	1.5	3/16	.018	O_2	7	69	------	281	2,560 ± 20
6	1.5	3/16	.018	O_2	8	69	------	277	2,520 ± 20
7	1.5	3/16	.018	Air	1	69	0.0069	248	2,520 ± 20
8	1.5	3/16	.018	Air	1	69	.0069	273	2,520 ± 20
9	1.5	3/16	.018	Air	4	69	.0069	281	2,520 ± 20
10	1.5	3/16	.018	Air	7	69	.0069	281	2,530 ± 20
11	1.5	3/16	.018	He	1	71	------	---	2,550 ± 15

[a]Model melted.

TABLE 21

TANK TESTS WITH INCONEL X

Run	Model specifications			Gas	Pressure, atm	Ambient temperature, °F	Humidity, lb H_2O / lb dry air	Power at failure, w	Brightness ignition temperature, °F (a)
	Length, in.	Width, in.	Thickness, in.						
1	1.5	3/16	0.025	O_2	1	69	------	284	2,500 ± 30
2	1.5	3/16	.025	O_2	1	69	------	277	2,500 ± 30
3	1.5	3/16	.025	O_2	3	69	------	298	2,550 ± 30
4	1.5	3/16	.025	O_2	5	69	------	302	2,560 ± 30
5	1.5	3/16	.025	O_2	7	69	------	295	2,530 ± 40
6	1.5	3/16	.025	O_2	8	69	------	307	2,510 ± 40
7	1.5	3/16	.025	Air	1	69	0.0072	284	2,455 ± 30
8	1.5	3/16	.025	Air	4	69	.0072	295	2,460 ± 30
9	1.5	3/16	.025	Air	7	69	.0072	288	2,480 ± 30
10	1.5	3/16	.025	He	1	72	------	---	2,550 ± 15

[a]Model melted.

TABLE 22

TANK TESTS WITH BERYLCO 25

Run	Model specifications			Gas	Pressure, atm	Ambient temperature, °F	Humidity, lb H_2O / lb dry air	Brightness ignition temperature, °F (a)
	Length, in.	Width, in.	Thickness, in.					
1	1.5	3/16	0.007	O_2	1	70	0.006	1,580
2	1.5	3/16	.007	O_2	1	70	.006	1,600
3	1.5	3/16	.007	O_2	3	70	.006	1,600
4	1.5	3/16	.007	O_2	5	70	.006	1,595
5	1.5	3/16	.007	O_2	7	70	.006	1,600
6	1.5	3/16	.007	Air	1	70	.006	1,600
7	1.5	3/16	.007	Air	4	70	.006	1,580
8	1.5	3/16	.007	Air	7	70	.006	1,585

[a]Model melted.

TABLE 23

TANK TESTS WITH BERYLCO 10

Run	Model Specifications			Gas	Pressure, atm	Ambient temperature, °F	Humidity, lb H_2O / lb dry air	Brightness ignition temperature, °F
	Length, in.	Width, in.	Thickness, in.					
1	1.5	1/4	0.015	O_2	1	70	-----	1,750
2	1.5	1/4	.015	O_2	1	70	-----	1,755
3	1.5	1/4	.015	O_2	3	70	-----	1,750
4	1.5	1/4	.015	O_2	5	70	-----	1,755
5	1.5	1/4	.015	O_2	7	70	-----	1,750
6	1.5	1/4	.015	Air	1	70	0.007	1,760
7	1.5	1/4	.015	Air	4	70	.007	1,760
8	1.5	1/4	.015	Air	7	70	.007	1,755

TABLE 24

RESULTS OF SHAPE EFFECT RUNS WITH CALCIUM CONES[a]

Run	Included angle, deg	Base diameter, in.	Air temperature, °F	Air velocity, ft/sec	Ignition temperature, °F
1	180	3/8	1,820	83	1,356
2	180	3/8	1,825	60	1,365
3	90	3/8	1,850	75	1,370
4	20	3/8	1,560	84	1,360
5	20	3/8	1,620	66	1,380
6	10	3/8	1,770	81	1,345
7	10	3/8	1,600	86	1,320
8	10	3/8	1,630	84	1,300
9	10	3/8	1,630	83	1,355

[a]99-percent pure calcium, turned from castings.

TABLE 25

PROPERTIES OF SOME METALS AND THEIR OXIDES

Metal	Oxide	Metal melting point, °C	Oxide melting point, °C	Volume ratio	Oxide density, g/cm³	γ, g oxide / g O_2	Heat of formation (18° C), cal/mole of oxide	Heat of reaction (18° C), cal/g of O_2
Be	BeO	1,278	2,520	1.68	3.01	1.562	[a]-66,000	[a]4,120
Mg	MgO	651	2,800	.81	3.58	2.52	-145,760	4,080
Ca	CaO	842	2,570	.64	3.37	3.44	-151,700	9,160
Th	ThO_2	1,845	2,950	1.35	10.03	8.25	-330,950	10,320
Ti	TiO_2	1,800	1,860	1.73	4.26	2.49	-217,000	6,680
Zr	ZrO_2	1,900	2,715	1.45	5.6	3.85	-178,700	5,580
V	V_2O_5	1,710	660	3.19	3.36	2.27	-437,200	5,560
Nb	NbO	1,950	-----	1.37	6.27	6.80	[a]-100,000	[a]6,300
Ta	Ta_2O_5	[b]3,027	1,470	2.54	8.74	5.52	-500,120	6,270
Cr	Cr_2O_3	1,890	2,440	2.07	5.2	3.17	-267,390	5,570
Mo	MoO_3	2,620	795	3.24	4.50	3.00	-174,000	3,650
W	WO_3	3,370	1,470	3.35	7.16	4.80	-191,400	3,970
Mn	Mn_3O_4	1,260	1,580	2.15	4.86	3.58	-327,840	5,130
Fe	FeO	1,535	1,371	.63	5.7	2.24	-64,040	2,000
	Fe_2O_3	1,535	1,565	2.14	5.24	3.32	-190,900	3,960
	Fe_3O_4	1,535	1,457	2.10	5.18	3.62	-265,950	4,150
Co	CoO	1,495	1,810	1.86	6.0	4.68	-57,490	3,600
Ni	NiO	1,455	1,960	1.65	7.45	4.67	-57,380	3,580
Cu	CuO	1,083	1,030	1.72	6.40	4.97	-31,800	1,980
Al	Al_2O_3	660	2,020	1.45	3.9	2.12	-339,050	7,060
Pb	PbO	327	885	1.26	9.53	13.95	-52,473	3,280
Ce	Ce_2O_3	640	1,692	1.16	7.0	6.85	-150,000	3,130
	CeO_2	640	3,000	1.22	7.3	10.78	-234,900	14,550
U	U_3O_8	[b]1,133	1,540	2.66	8.30	6.58	-845,170	6,600

[a]Unreliable data.

[b]Dissociates.

TABLE 26

OXIDATION AND IGNITION DATA OF MAGNESIUM ALLOYS

[Data obtained from references 7 and 8]

Alloy metal, percent by weight	A_l, g/cm^2-sec	E_l, cal/mole	T_{ig}, °F
1.78% Al	2.5×10^4	42,700	1,105
3.81% Al	3.1×10^3	38,600	1,065
7.23% Al	7.5×10^8	54,700	1,018
9.12% Al	1.1×10^{16}	74,500	990
1.54% Zn	3.1×10^6	50,000	1,076
3.28% Zn	2.7×10^1	31,500	1,045
3.83% Ag	1.1×10^7	52,600	1,049
3.78% Sn	3.3×10^1	31,600	1,112
3.86% In	2.3×10^5	46,600	1,148
4.18% Cd	1.7×10^6	50,500	1,148
3.94% Pb	7.5×10^6	51,600	1,112
.49% Ni	9.7×10^4	42,000	1,085
.23% Cu	6.6×10^5	44,800	1,148

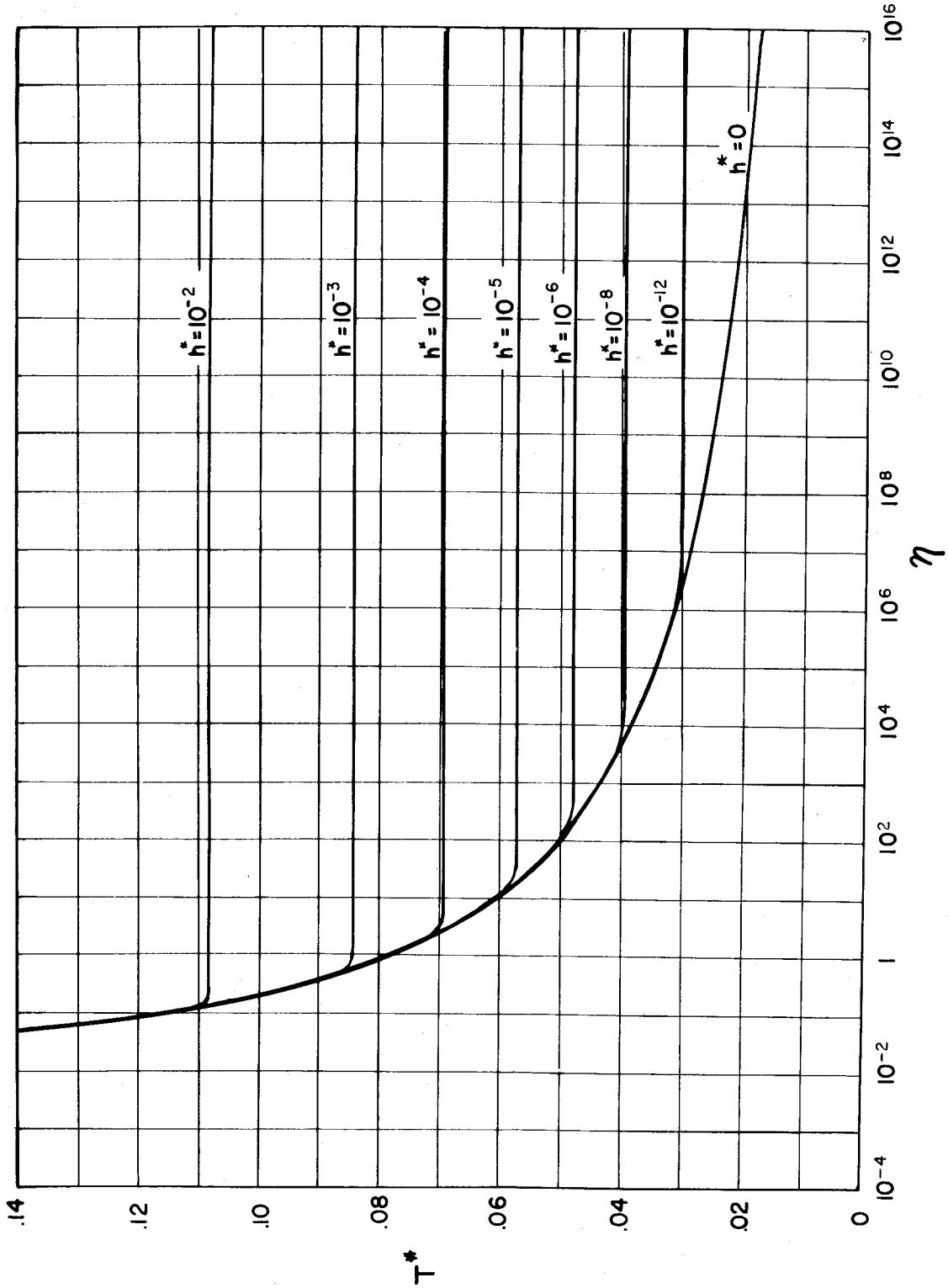

Figure 1.- Curves for prediction of ignition temperatures from oxidation data.

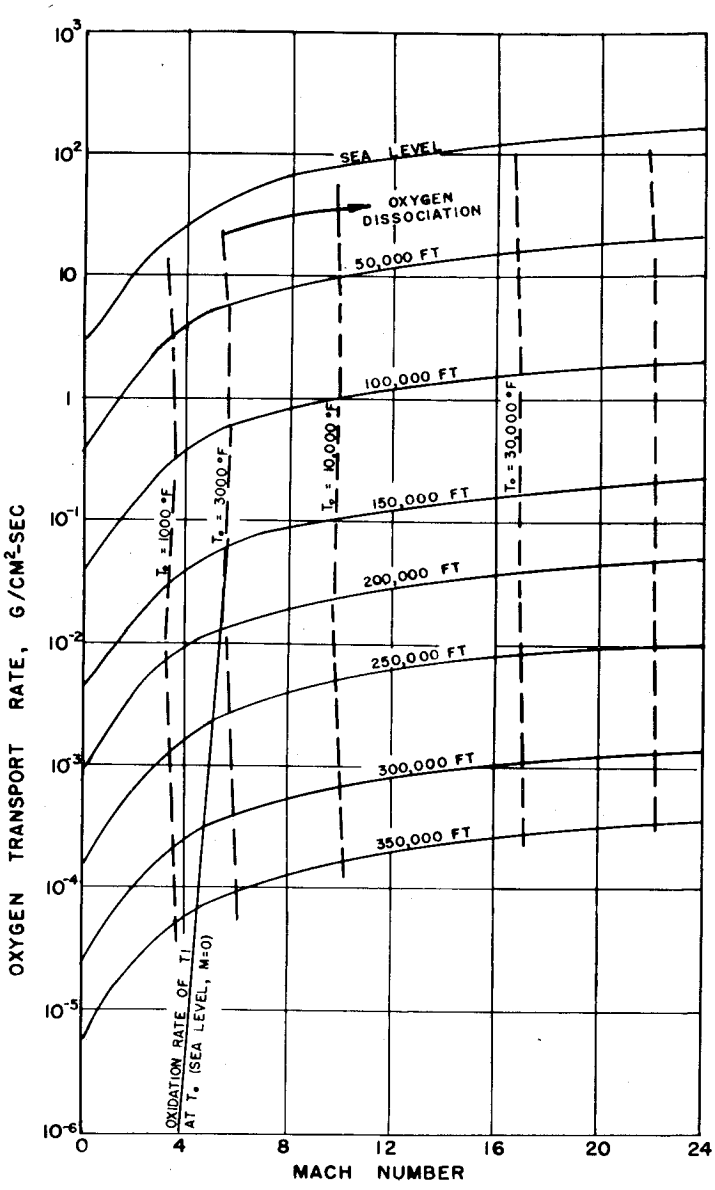

Figure 2.- Oxygen transport rate behind a normal shock wave.

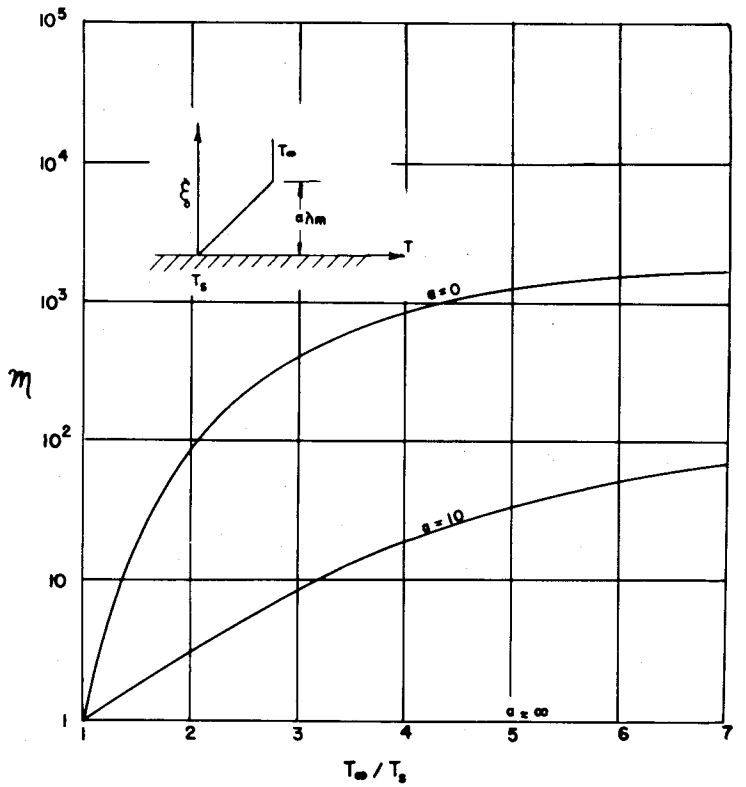

Figure 3.- Dependence of adsorption rate on temperature variation near surface. $\frac{E}{RT_S} = 10$; $\frac{dw}{d\theta} = \eta\left(\frac{dw}{d\theta}\right)_{iso}$.

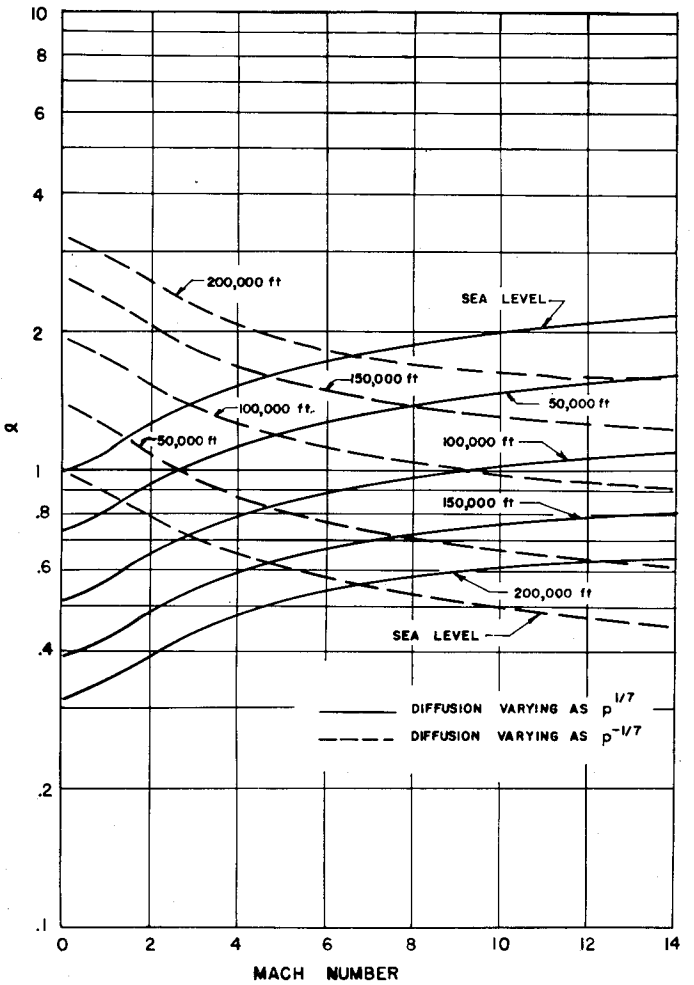

Figure 4.- Effect of flight conditions on rates of diffusion through oxide film. $\frac{dw}{d\theta} = \alpha\left(\frac{dw}{d\theta}\right)_{\text{sea level,M=0}}$.

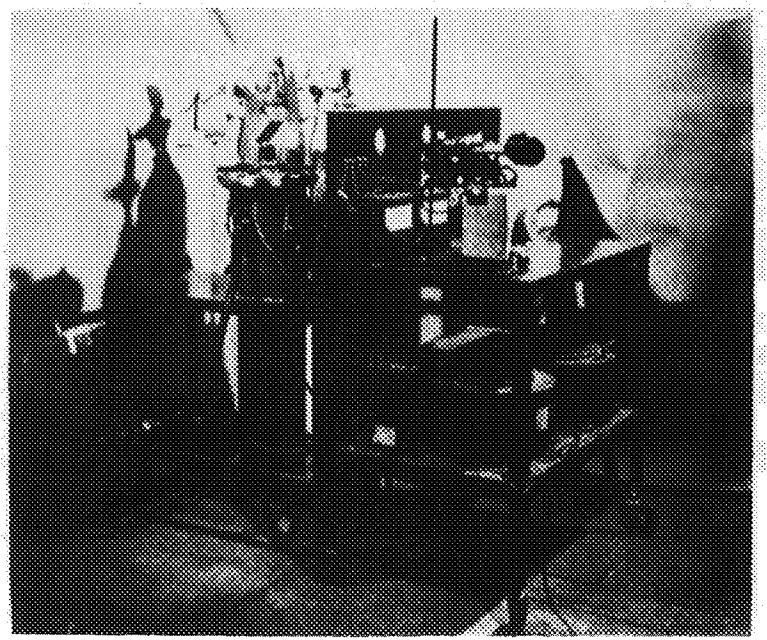

L-58-100a
Figure 5.- Pressure tank and control console.

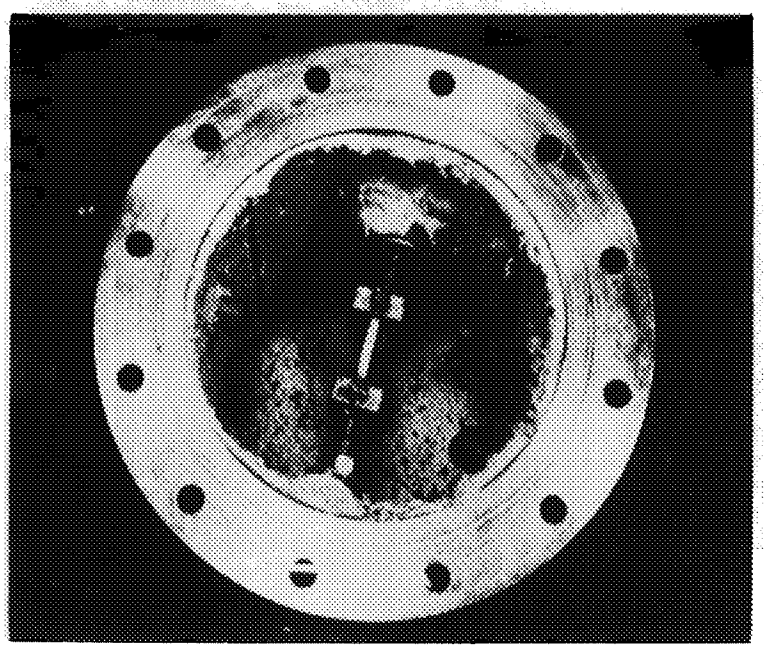

L-58-101a
Figure 6.- Inside of pressure tank.

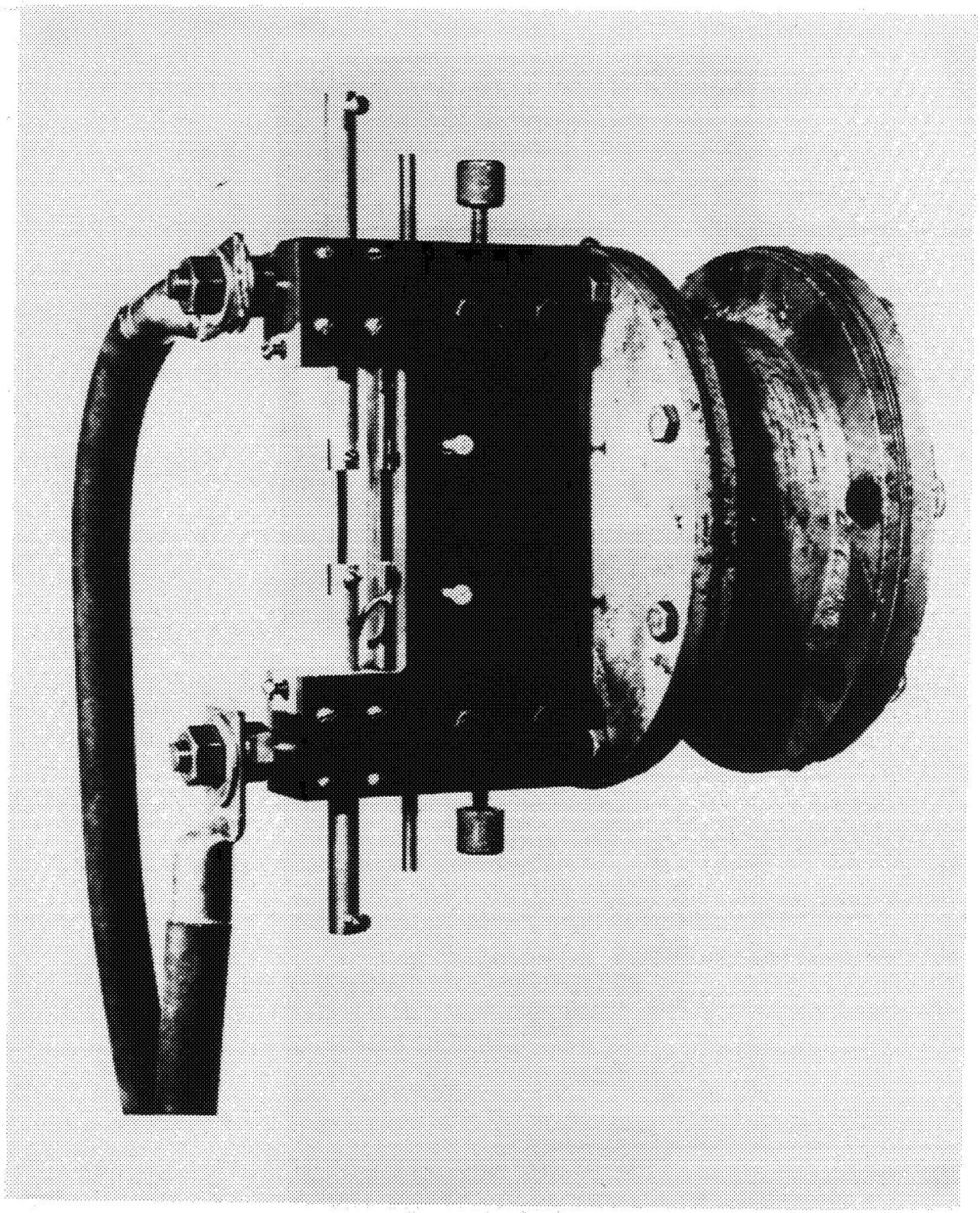

Figure 7.- Wind-tunnel apparatus. L-58-102a

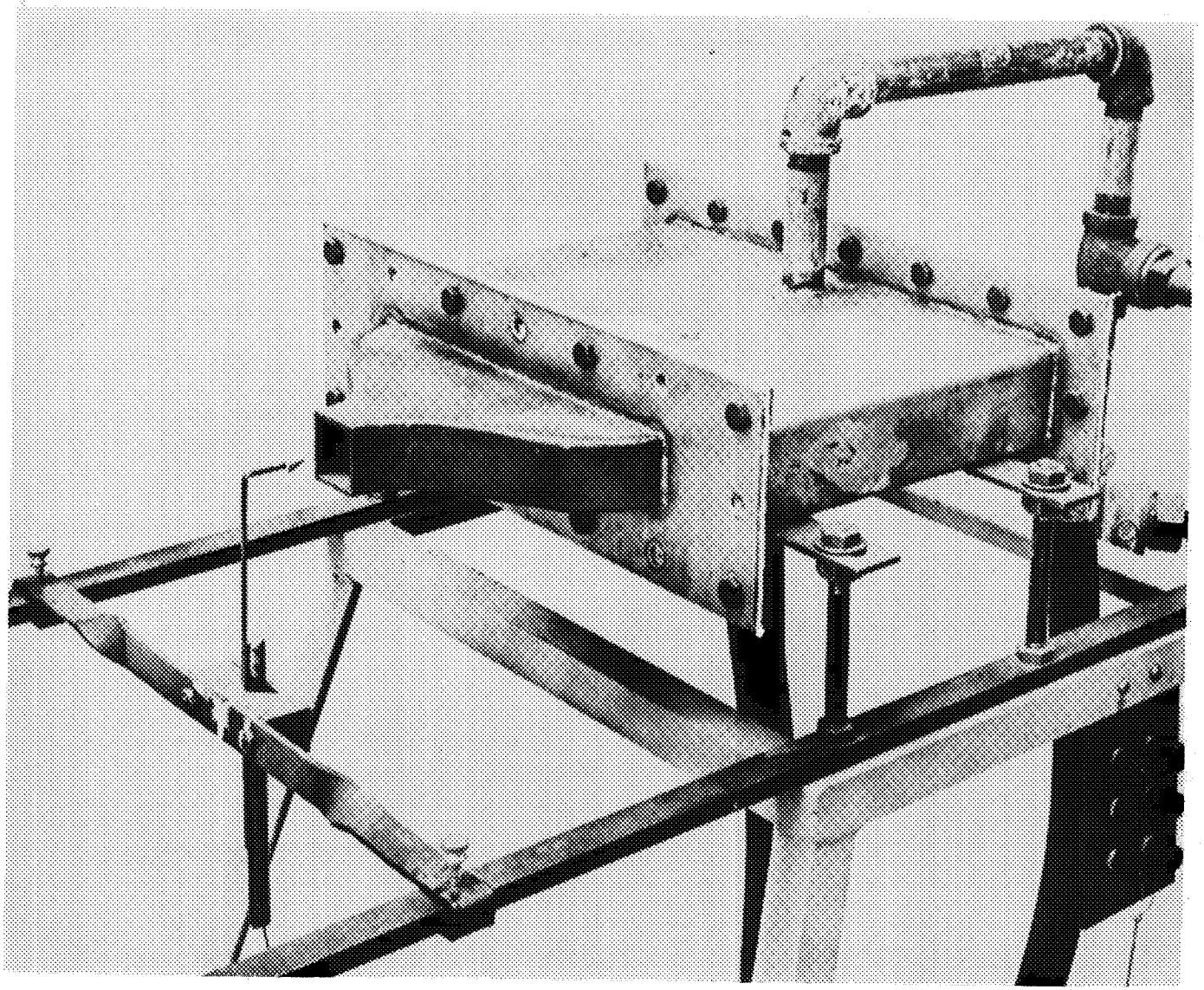

Figure 8.- Hot-air apparatus. L-58-103a

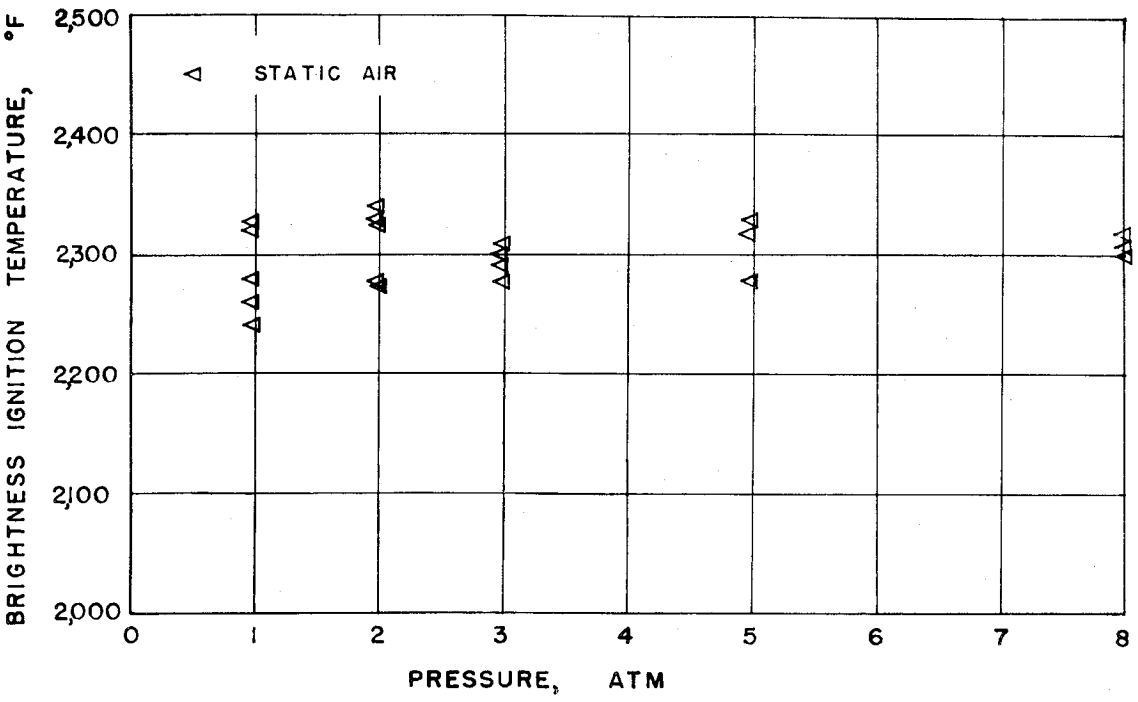

Figure 9.- Ignition temperatures of mild steel.

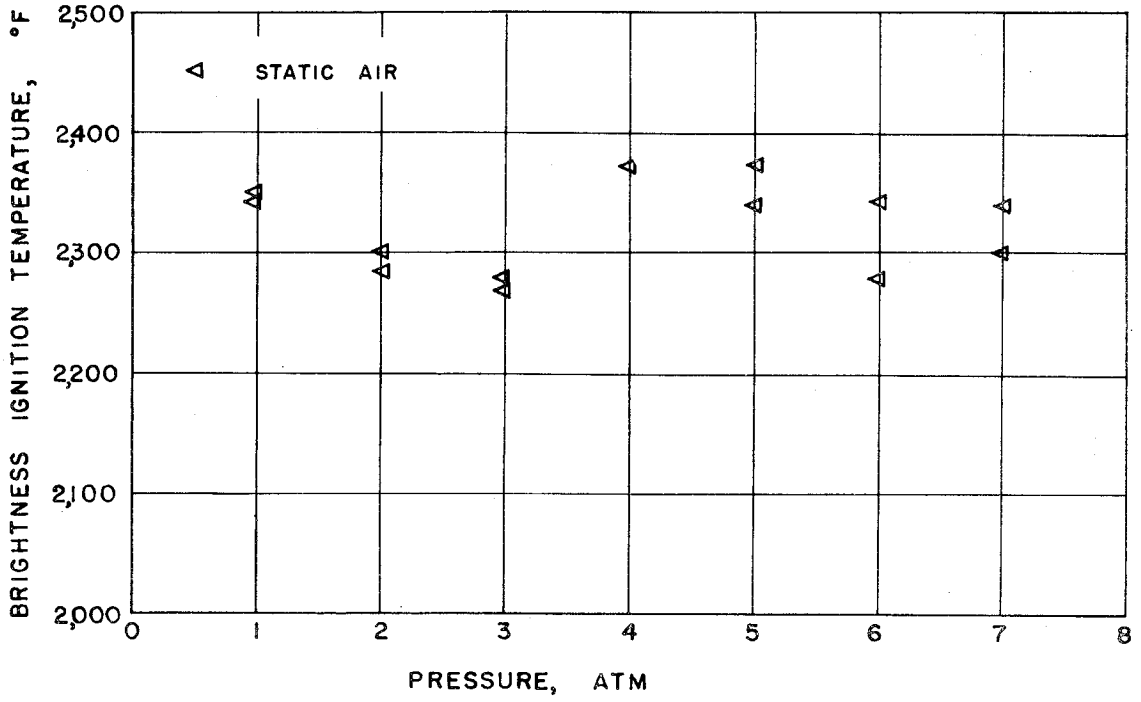

Figure 10.- Ignition temperatures of tungsten.

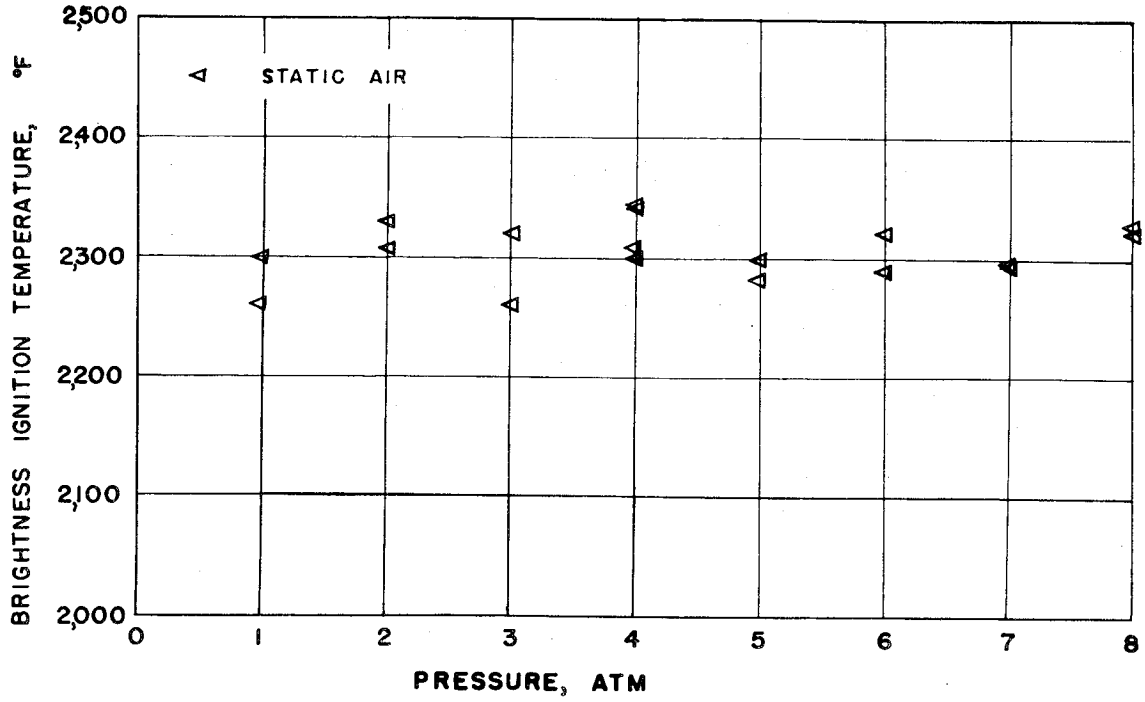

Figure 11.- Ignition temperatures of tantalum.

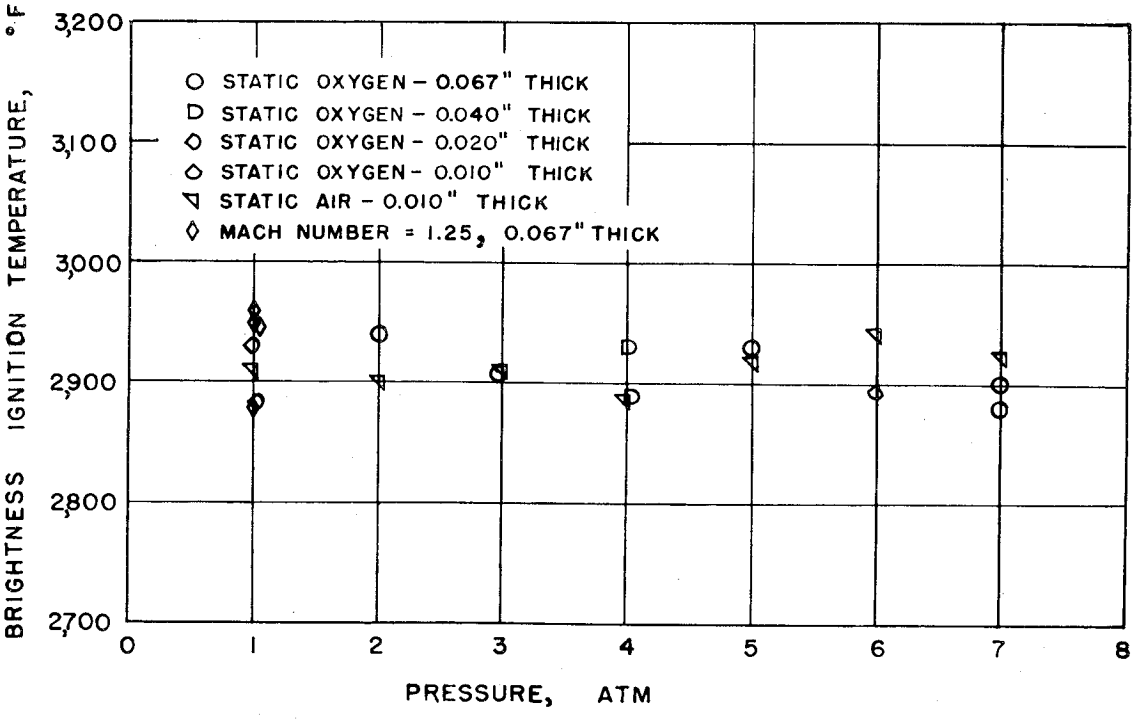

Figure 12.- Ignition temperatures of titanium RC-70.

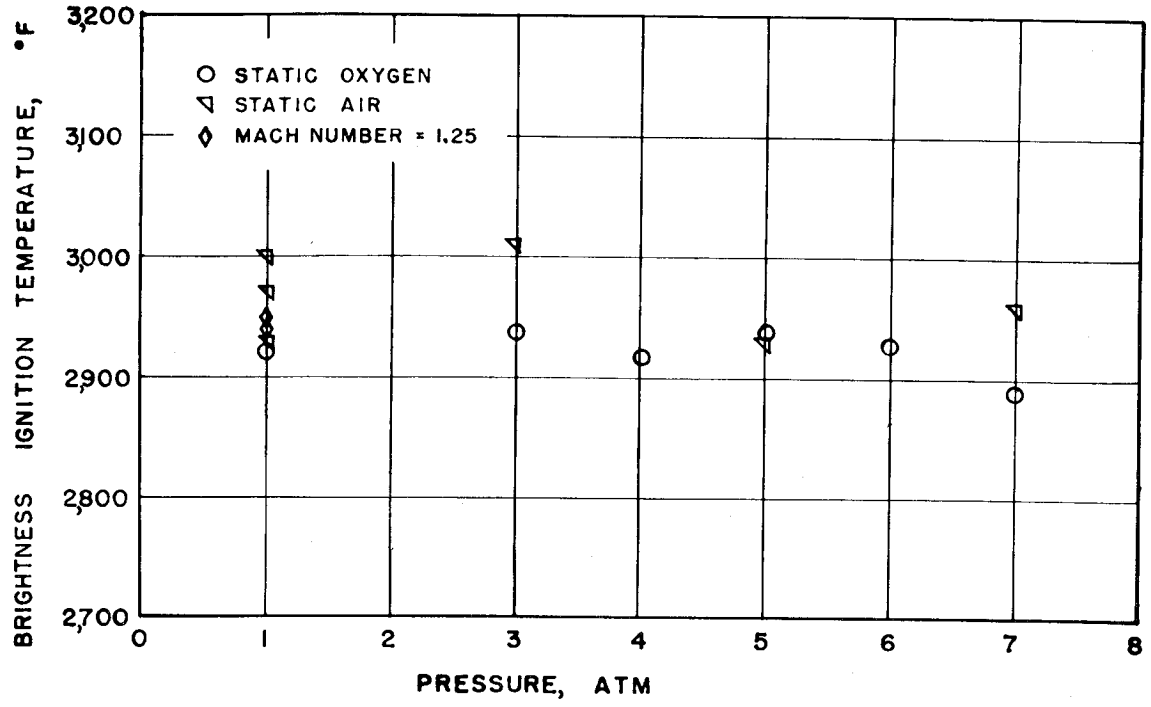

Figure 13.- Ignition temperatures of titanium RS-70.

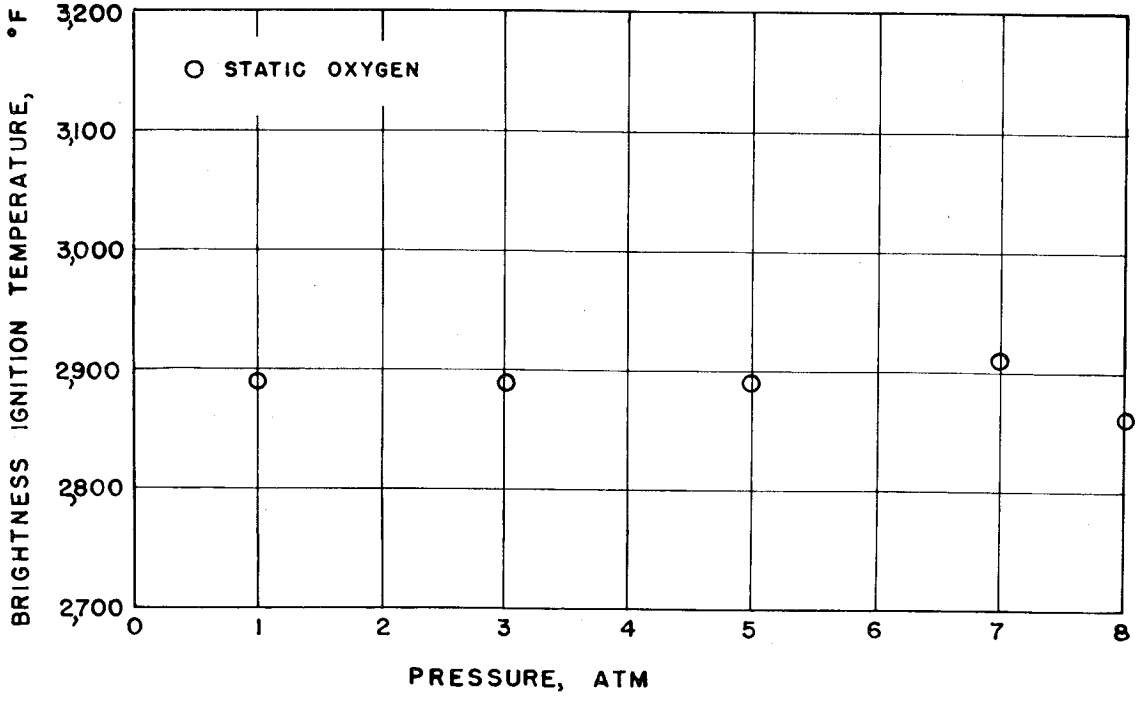

Figure 14.- Ignition temperatures of titanium RS-110-A.

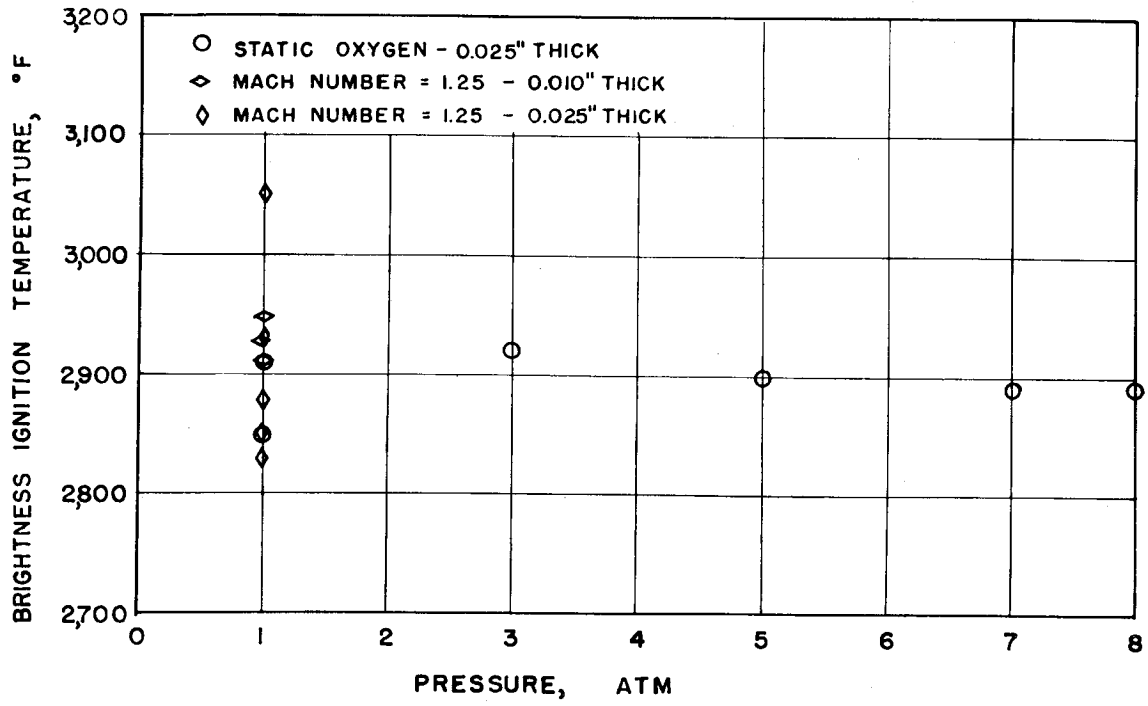

Figure 15.- Ignition temperatures for titanium RS-110-BX.

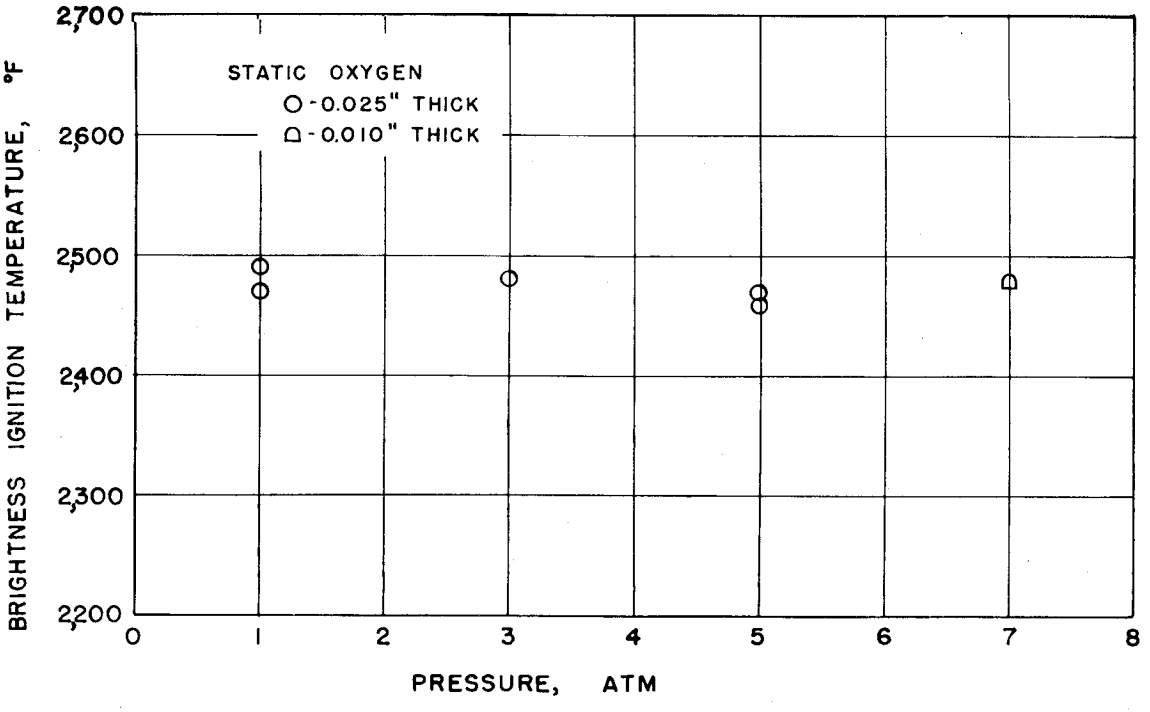

Figure 16.- Ignition temperatures of stainless steel 430.

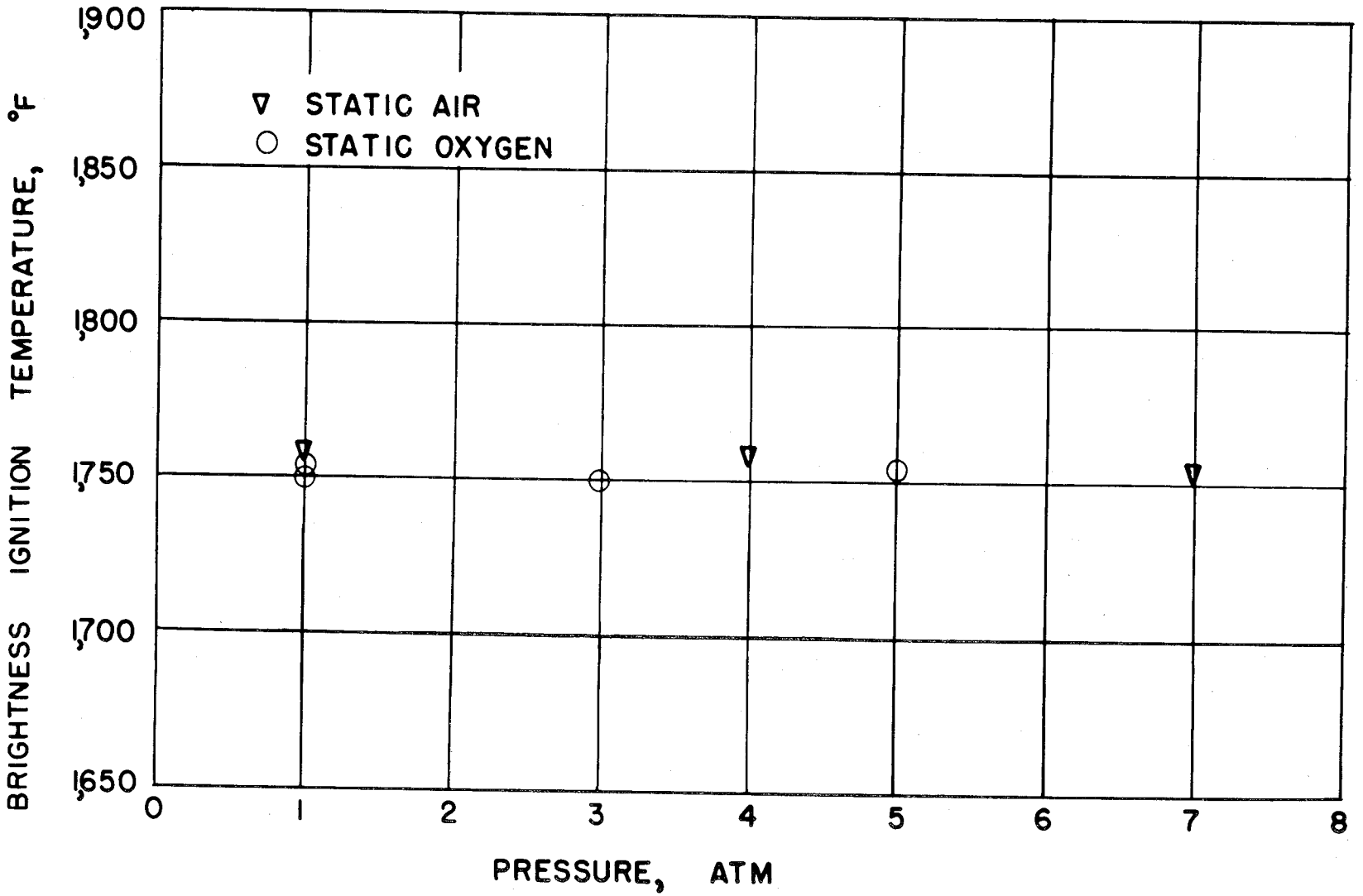

Figure 17.- Ignition temperatures of Berylco 10.

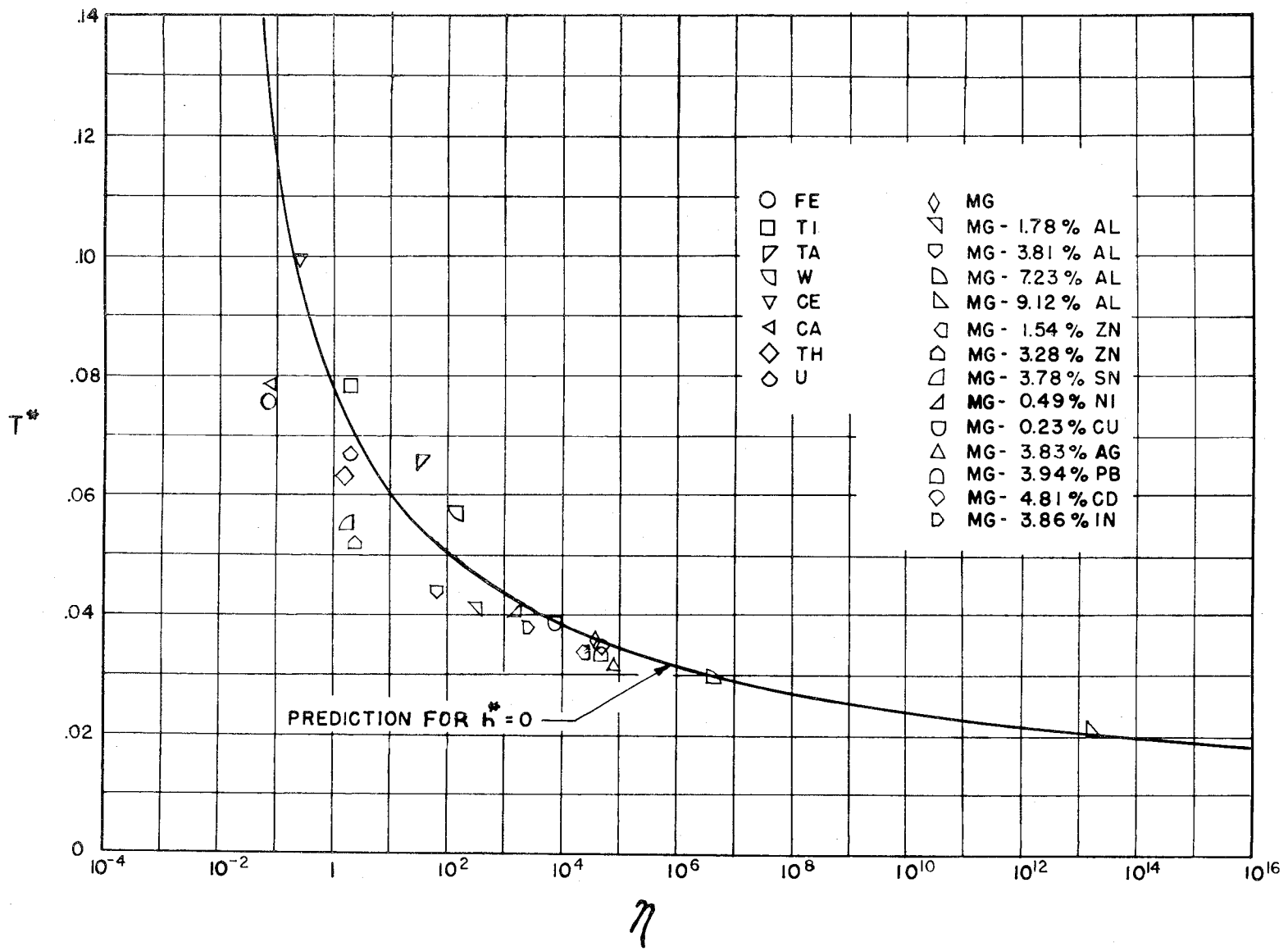

Figure 18.- Comparison of predicted and experimental ignition temperatures.

NASA TN D-182
National Aeronautics and Space Administration.
INVESTIGATION OF IGNITION TEMPERATURES OF SOLID METALS. W. C. Reynolds, Stanford University. October 1959. 71p. diagrs., photos., tabs. OTS price, $2.00. (NASA TECHNICAL NOTE D-182)

The ignition temperature of a solid metal is related through a thermal definition of ignition to the rate of oxidation and to the radiation and convection heat-transfer parameters. The mechanisms of oxidation are reviewed and the factors which influence ignition temperatures are discussed. Reasonable agreement between theoretical and experimental ignition temperatures is demonstrated. Experimental ignition temperatures for several metals are presented.

Copies obtainable from NASA, Washington

1. Heat, Additions of - Aerodynamic (1.1.4.3)
2. Heat Transfer, Theory and Experiment (3.9.1)
3. Materials, Properties - Thermal (5.2.11)

I. Reynolds, W. C.
II. NASA TN D-182
III. Stanford U.

NASA

NASA TN D-182
National Aeronautics and Space Administration.
INVESTIGATION OF IGNITION TEMPERATURES OF SOLID METALS. W. C. Reynolds, Stanford University. October 1959. 71p. diagrs., photos., tabs. OTS price, $2.00. (NASA TECHNICAL NOTE D-182)

The ignition temperature of a solid metal is related through a thermal definition of ignition to the rate of oxidation and to the radiation and convection heat-transfer parameters. The mechanisms of oxidation are reviewed and the factors which influence ignition temperatures are discussed. Reasonable agreement between theoretical and experimental ignition temperatures is demonstrated. Experimental ignition temperatures for several metals are presented.

Copies obtainable from NASA, Washington

1. Heat, Additions of - Aerodynamic (1.1.4.3)
2. Heat Transfer, Theory and Experiment (3.9.1)
3. Materials, Properties - Thermal (5.2.11)

I. Reynolds, W. C.
II. NASA TN D-182
III. Stanford U.

NASA

NASA TN D-182
National Aeronautics and Space Administration.
INVESTIGATION OF IGNITION TEMPERATURES OF SOLID METALS. W. C. Reynolds, Stanford University. October 1959. 71p. diagrs., photos., tabs. OTS price, $2.00. (NASA TECHNICAL NOTE D-182)

The ignition temperature of a solid metal is related through a thermal definition of ignition to the rate of oxidation and to the radiation and convection heat-transfer parameters. The mechanisms of oxidation are reviewed and the factors which influence ignition temperatures are discussed. Reasonable agreement between theoretical and experimental ignition temperatures is demonstrated. Experimental ignition temperatures for several metals are presented.

Copies obtainable from NASA, Washington

1. Heat, Additions of - Aerodynamic (1.1.4.3)
2. Heat Transfer, Theory and Experiment (3.9.1)
3. Materials, Properties - Thermal (5.2.11)

I. Reynolds, W. C.
II. NASA TN D-182
III. Stanford U.

NASA

NASA TN D-182
National Aeronautics and Space Administration.
INVESTIGATION OF IGNITION TEMPERATURES OF SOLID METALS. W. C. Reynolds, Stanford University. October 1959. 71p. diagrs., photos., tabs. OTS price, $2.00. (NASA TECHNICAL NOTE D-182)

The ignition temperature of a solid metal is related through a thermal definition of ignition to the rate of oxidation and to the radiation and convection heat-transfer parameters. The mechanisms of oxidation are reviewed and the factors which influence ignition temperatures are discussed. Reasonable agreement between theoretical and experimental ignition temperatures is demonstrated. Experimental ignition temperatures for several metals are presented.

Copies obtainable from NASA, Washington

1. Heat, Additions of - Aerodynamic (1.1.4.3)
2. Heat Transfer, Theory and Experiment (3.9.1)
3. Materials, Properties - Thermal (5.2.11)

I. Reynolds, W. C.
II. NASA TN D-182
III. Stanford U.

NASA

NASA TN D-182
National Aeronautics and Space Administration.
INVESTIGATION OF IGNITION TEMPERATURES OF SOLID METALS. W. C. Reynolds, Stanford University. October 1959. 71p. diagrs., photos., tabs. OTS price, $2.00. (NASA TECHNICAL NOTE D-182)

The ignition temperature of a solid metal is related through a thermal definition of ignition to the rate of oxidation and to the radiation and convection heat-transfer parameters. The mechanisms of oxidation are reviewed and the factors which influence ignition temperatures are discussed. Reasonable agreement between theoretical and experimental ignition temperatures is demonstrated. Experimental ignition temperatures for several metals are presented.

Copies obtainable from NASA, Washington

1. Heat, Additions of - Aerodynamic (1.1.4.3)
2. Heat Transfer, Theory and Experiment (3.9.1)
3. Materials, Properties - Thermal (5.2.11)

I. Reynolds, W. C.
II. NASA TN D-182
III. Stanford U.

NASA

NASA TN D-182
National Aeronautics and Space Administration.
INVESTIGATION OF IGNITION TEMPERATURES OF SOLID METALS. W. C. Reynolds, Stanford University. October 1959. 71p. diagrs., photos., tabs. OTS price, $2.00. (NASA TECHNICAL NOTE D-182)

The ignition temperature of a solid metal is related through a thermal definition of ignition to the rate of oxidation and to the radiation and convection heat-transfer parameters. The mechanisms of oxidation are reviewed and the factors which influence ignition temperatures are discussed. Reasonable agreement between theoretical and experimental ignition temperatures is demonstrated. Experimental ignition temperatures for several metals are presented.

Copies obtainable from NASA, Washington

1. Heat, Additions of - Aerodynamic (1.1.4.3)
2. Heat Transfer, Theory and Experiment (3.9.1)
3. Materials, Properties - Thermal (5.2.11)

I. Reynolds, W. C.
II. NASA TN D-182
III. Stanford U.

NASA

NASA TN D-182
National Aeronautics and Space Administration.
INVESTIGATION OF IGNITION TEMPERATURES OF SOLID METALS. W. C. Reynolds, Stanford University. October 1959. 71p. diagrs., photos., tabs. OTS price, $2.00. (NASA TECHNICAL NOTE D-182)

The ignition temperature of a solid metal is related through a thermal definition of ignition to the rate of oxidation and to the radiation and convection heat-transfer parameters. The mechanisms of oxidation are reviewed and the factors which influence ignition temperatures are discussed. Reasonable agreement between theoretical and experimental ignition temperatures is demonstrated. Experimental ignition temperatures for several metals are presented.

Copies obtainable from NASA, Washington

1. Heat, Additions of - Aerodynamic (1.1.4.3)
2. Heat Transfer, Theory and Experiment (3.9.1)
3. Materials, Properties - Thermal (5.2.11)

I. Reynolds, W. C.
II. NASA TN D-182
III. Stanford U.

NASA

NASA TN D-182
National Aeronautics and Space Administration.
INVESTIGATION OF IGNITION TEMPERATURES OF SOLID METALS. W. C. Reynolds, Stanford University. October 1959. 71p. diagrs., photos., tabs. OTS price, $2.00. (NASA TECHNICAL NOTE D-182)

The ignition temperature of a solid metal is related through a thermal definition of ignition to the rate of oxidation and to the radiation and convection heat-transfer parameters. The mechanisms of oxidation are reviewed and the factors which influence ignition temperatures are discussed. Reasonable agreement between theoretical and experimental ignition temperatures is demonstrated. Experimental ignition temperatures for several metals are presented.

Copies obtainable from NASA, Washington

1. Heat, Additions of - Aerodynamic (1.1.4.3)
2. Heat Transfer, Theory and Experiment (3.9.1)
3. Materials, Properties - Thermal (5.2.11)

I. Reynolds, W. C.
II. NASA TN D-182
III. Stanford U.

NASA